ADSORPTIVE REMOVAL OF FURFURAL IN PACKED COLUMN

A DISSERTATION

Submitted in partial fulfillment of the requirements for the award of the degree of

MASTER OF TECHNOLOGY

in

CHEMICAL ENGINEERING

(With Specialization in Industrial Pollution Abatement)

By

SAURABH SINGH

DEPARTMENT OF CHEMICAL ENGINEERING
INDIAN INSTITUTE OF TECHNOLOGY ROORKEE
ROORKEE - 247 667 (INDIA)

JUNE, 2008

INDIAN INSTITUTE OF TECHNOLOGY ROORKEE
ROORKEE
CANDIDATE'S DECLARATION

I hereby declare that the work, which is being presented in the dissertation entitled **"ADSORPTIVE REMOVAL OF FURFURAL IN PACKED COLUMN"**, in the partial fulfilment of the requirements of the award of the degree of Master of Technology in Chemical Engineering with specialization in Industrial Pollution Abatement, submitted in the Department of Chemical Engineering, Indian Institute of Technology Roorkee, Roorkee, Uttarakhand (India), is an authentic record of my own work carried out during the period from June 2007 to June 2008 under supervision of Dr. I. D. Mall, Professor, and Dr. V.C. Srivastava, Lecturer, Department of Chemical Engineering, Indian Institute of Technology Roorkee, Roorkee.

I have not submitted the matter, embodied in this dissertation for the award of any other degree or diploma.

Date: 30 June, 2008

Place: Roorkee

Saurabh Singh

SAURABH SINGH

CERTIFICATE

This is to certify that the above statement made by the candidate is correct to the best of my knowledge and belief.

(Dr. I. D. Mall)
Professor
Department of Chemical Engineering
IIT Roorkee
Roorkee, Uttarakhand - 247 667

Vinod Chandra Srivastava

(Dr. V.C. Srivastava)
Lecturer
Department of Chemical Engineering
IIT Roorkee
Roorkee, Uttarakhand - 247 667

ACKNOWLEDGEMENT

I express my deep sense of gratitude to my guide **Dr. I. D. Mall**, Professor, and **Dr. Vimal Chand Srivastava,** Lecturer, Department of Chemical Engineering, Indian Institute of Technology Roorkee, for his keen interest, constant guidance and encouragement throughout the course of this dissertation, his experience, assiduity and deep insight of the subject held this work always on a smooth and steady course. Useful criticism and constant help extended in the hours of need had been immensely useful.

I would like to thanks to Dr. Shri Chand, Professor and Head, Department of Chemical Engineering, Indian Institute of Technology Roorkee, Roorkee, for providing various facilities during this work.

I also would like to thanks to Mr. Rajendra Bhatnagar (Senior Laboratory Assistant) Shri Ayodhya Prasad (Senior Laboratory Attendant), Pollution Abatement Research Laboratory and Ekka (Workshop incharge), Department of Chemical Engineering, IIT Roorkee, for their continuous help during the experimental work.

I am greatly indebted to all of my seniors and friends for their enthusiastic support, encouragement and help, made me come up with this report.

I thank all well wishers who in any manner directly or indirectly have put a helping hand in any part of this piece of work.

Above all, I want to express my heartiest gratitude to all my family members for their love, faith and support for me, which has always been a constant source of inspiration.

SAURABH SINGH

ABSTRACT

In previous study, activated carbon commercial grade (ACC) and bagasse fly ash (BFA) were used as adsorbents for the removal of furfural in batch adsorption study [Sahu et al., 2008 a, b]. The present study was carried out to evaluate the performance of ACC and BFA packed column for adsorptive removal of furfural from aqueous solution. The effect of various parameters like bed height (Z = 15-60 cm), flow rate (Q = 0.02-0.04 L/min), initial concentration of furfural (C_o = 50-200 mg/L) and column diameter (D=2-4 cm) on the breakthrough curve of furfural adsorption were investigated. Adams–Bohart, Bed-Depth Service-Time, Thomas, Yoon–Nelson, Clark and Wolborska models were applied to the experimental data for the prediction of the breakthrough point, and to determine the characteristic parameters of the column. Error analysis showed that the Yoon–Nelson model best described the experimental breakthrough curve, while Wolborska model showed good prediction of breakthrough curve for the relative concentration region up to 0.5 for furfural adsorption in ACC packed column. For BFA packed column, Thomas model well represented the experimental data points under all experimental conditions. It was obserbed that both ACC and BFA can be utilized efficiently in continuous system for the removal of furfural.

Overall, BFA packed column showed higher removal efficiency as compared to ACC packed column at all Q, Z and C_o.

CONTENTS

LIST OF TABLES

LIST OF FIGURES

NOMENCLATURE

A_C	cross-sectional area of the column (cm^2)
ACC	Activated carbon commercial grade
a_R	Constant of Redlich-Peterson isotherm (L/mg)
BFA	Bagasse fly ash
C	concentration of the solute at time t (mg/L)
C_e	Concentration of adsorbate solution at equilibrium (mg/L)
C_0	initial concentration of the solute (mg/L)
C_b	concentration of the solute at breakthrough time t_b (mg/L)
$EBCT$	empty bed contact time
I	intercept of Eq. (3.17)
k	adsorption rate constant for the column (L/min mg)
k_0	Constant in Bangham equation
k_f	Rate constant of pseudo-first-order adsorption model (L/min)
k_T	Thomas rate constant (L/min mg)
k_{id}	Intra-particle diffusion rate constant (mg/g min $L^{1/2}$)
k_{YN}	Yoon-Nelson rate constant (min^{-1})
K_F	Constant of Freundlich isotherm, (mg/g)/(L /mg)$^{1/n}$
K_L	Constant of Langmuir isotherm, L/mg
K_R	Constant of Redlich-Peterson isotherm, L/g
K_T	Temkin isotherm constant, (L/mg)
m_C	mass of adsorbent in the column (g)
q_m	Maximum adsorption capacity of adsorbent, mg/g
n	Freundlich constant
N	number of data points
N_0	adsorptive capacity of adsorbent (mg/L)
N_b	bed volumes to breakthrough

P	number of parameters
Q	volumetric flow rate (L/min)
Q_0	maximum solid-phase concentration of the solute (mg/g)
r	a parameter in Clark model (min^{-1})
t	time of contact time (min)
t_b	time for adsorbate breakthrough (min)
$t_{0.5}$	time for 50% adsorbate breakthrough (min)
U	linear flow velocity of the feed to the bed (m/min)
U_r	adsorbent usage rate (g/L)
V_b	volume of solution treated at breakthrough (L)
V_C	volume of the adsorbent in the bed (L)
V_{eff}	throughput volume (L)
Z	depth of the column bed (m)
ε	percent deviation between the experimental and theoretical time for the breakthrough
β	kinetic coefficient of the external mass transfer (min^{-1})
ρ	apparent density of adsorbent in column (g/cm^3)
v_m	migration velocity of the concentration front in the bed (cm/min)
$MPSD$	Marquardt's Percent Standard Deviation

Greek symbols

α	Bangham constant (<1)
β	Constant of Redlich-Peterson isotherm ($0<\beta<1$)

Chapter – I

INTRODUCTION

1.1 GENERAL

The release of complex chemicals from oil refineries, petrochemical industries, , oil processing and chemical plants into the environment has been considered as a major source of air and water pollution. Many of these materials are non-biodegradable or inhibitors for biological systems and often have a toxic effect on life systems. In natural environment they have a long life and are slow to decay and decompose. Some cyclic and aromatic organic compound such as phenols and furfural are very toxic and are considered as a serious problem for environment.

Furfural is a polar solvent used extensively in lube oil refining operations as extraction solvent for extracting aromatic hydrocarbons from raw lube distillates thereby improving the viscosity temperature characteristics and oxidation stability of the lube base stocks. Furfural extraction unit experiences furfural loss in the effluent water streams. Furfural is an irritant of the skin, mucous membranes and respiratory tract. Concentration of 1.9 to 14 mg/L produces symptoms of such irritation in exposed workers. Apart from being an environmental pollution problem, this leakage also constitutes a sizable economic loss. Therefore it is necessary to recover the lost furfural. This loss is especially significant in large lube units, which may lose up to 2 wt % furfural in effluent water streams. The recovery of furfural from aqueous waste is also of importance in paper Industry as furfural is byproduct of wood decomposition. Solvent extraction may be used to recover furfural from wastewater, however there are constraints in the solvent recovery and solvent solubility in the water streams. Furfural

also has been identified as one of the main components of smoke condensates of pine and cottonwood. It was a major constituent of glowing fires of conifer logs. Residential burning of brown-coal briquettes led to emission of furfural, at an emission factor of 1.63 mg/kg. The estimated total amount of furfural emitted in the city of Leipzig was 530 kg/year. Furfural has been measured at a concentration of 0.19 mg/m^3 at the foot of Mount Everest in Nepal (IARC, 1995).

Furfural also gets formed during the thermal decomposition of carbohydrates, and is thus found in numerous processed food and beverage products. It is also carried over into food from its use as an extraction solvent or as a component of flavour mixtures. The highest reported concentrations were found in wheat bread (0.8-14 mg/kg), cognac (0.6-33 mg/kg), rum (22 mg/kg), malt whisky (10-37 mg/kg), port wine (2-34 mg/kg), and coffee (55-255 mg/kg). The concentrations of furfural in juices were 0.01-4.94 mg/kg (IARC, 1995; JECFA, 1993).

1.2 FURFURAL: MAJOR SOURCES & PROPERTIES

Furfural is an aromatic aldehyde, with the cyclic structure shown in Fig 1.1 Furfural derived from a variety of agricultural byproducts, including corncobs, oat and wheat bran, and sawdust. It is also produced in pulp and paper industry in wood pulping process. Its chemical formula is $C_5H_4O_2$. In its pure state, it is a colorless oily liquid with the odor of almonds, but upon exposure to air it quickly becomes yellow. Physical properties of furfural have listed in the Table 1.1. Furfural dissolves readily in most polar organic solvents, but is only slightly soluble in either water or alkanes. Furfural is a clear, colourless motile liquid.

1.2.1 INDUSTRIAL APPLICATION

It has a wide application in petroleum refining, petrochemical, pharmaceutical industries and food industry. The major applications of furfural are as follows:

- As a excellent organic solvent in Lube oil refining to extract dienes and other impurities from hydrocarbons,
- As a bonding agent in the manufacture of grinding wheels and abrasives,
- In manufacture of phenolic resins as an ingredient,
- As a solvent (for nitrated cotton, cellulose acetate and gums), to accelerate vulcanization,
- As an intermediate in the synthesis of furan derivatives,
- As a weed killer, and as a fungicide,
- Furfural is also used as a flavouring agen.

Some important industrial application of furfural are summarized in Table 1.2.

1.2.2 CONSUMPTION

The demand estimates for furfural for its various applications developed in India are as given in Table 1.3. Considering the capacity of existing units and the new capacity, mostly by way of new units likely to materialise in future, the demand and supply situation has been estimated as given in Table 1.4.

From the inception of the industry, furfural manufacturing activity in the country has been dependent on foreign technology. Two manufacturers have imported plant and machinery and process know-how from internationally leading manufacturers of furfural.

The heavy dependence on borrowed technology indicates that continuous efforts towards development have not yielded the desired results. Moreover, in spite of borrowed technology the Indian industry generally has not achieved its goals. Research and development appears to be inadequate in the furfural industry. Efforts to develop end-use applications need to be stepped up.

1.2.3 PRODUCTION

Furfural is prepared industrially from pentosans present in cereal straws and brans by hydrolysis and dehydration with strong inorganic acids. As no commercial synthetic routes have been found so far, all furfural manufacturing activity is based on pentosan containing residues that are obtained from the processing of various agricultural and forest products. Furfural is produced from biomass containing pentose, a short chain sugar found in corn cobs, sugar cane bagasse, rice and oat hulls etc. Many plant materials contain the polysaccharide hemicellulose, a polymer of sugars containing five carbon atoms each. When heated with sulfuric acid, hemicellulose undergoes hydrolysis to yield these sugars, principally xylose. Under the same conditions of heat and acid, xylose and other five carbon sugars undergo dehydration, losing three water molecules to become furfural:

$$C_5H_{10}O_5 \rightarrow C_5H_4O_2 + 3\ H_2O$$

For crop residue feedstocks, about 10% of the mass of the original plant matter can be recovered as furfural. Furfural and water evaporate together from the reaction mixture, and separate upon condensation. The manufacturing activity in the country started in the 70's with the Southern Agrofurane Industries Ltd. At present, in India, there are only three units manufacturing furfural. Out of these three units only one unit is manufacturing furfural using Bagasse as a raw material and the other two units are

using rice husk. Table 1.5 presents some manufacturers of furfural in India. The installed capacity of the industry during 1988-89 was 6400 tonnes per annum. As against this the production was about 1148 tonnes. The utilisation of capacity has been estimated at 18%.

World production of furfural is wholly based on agro-industrial residues or wastes that are abundantly available in many developing countries and are often under-utilized or unexploited. Production technologies have been developed to suit the various types of raw materials found in these countries. Global total capacity of production is about 450,000 ton. China is the biggest supplier of this product and they have about a half of global capacity. In China, Furfural is produced from corn cobs in the Northern Provinces. There are a number of small plants and also several large ones particularly in Shandong Province.

1.3 TOXICITY OF FURFURAL

The highest reported emissions of furfural to the environment are from the wood pulp industry and lubricating oil processing unit, whereas its release to water from other uses is substantially lower. Levels reported in food are as follows: non-alcoholic beverages, 4 mg/l; alcoholic beverages, 10 mg/l; ice creams, 13 mg/kg; candy, 12 mg/kg; baked goods, 17 mg/kg; gelatins and puddings, 0.8 mg/kg; chewing gum, 45 mg/kg; and syrups, 30 mg/l [CICAD, 2000].

Furfural is an irritant to the skin, eyes, mucous membranes, and respiratory tract. It acts as a toxicant to the central nervous system, liver, kidney, blood, and bone marrow. The oral LD_{50} in rats is 65 mg/kg; and the inhalation LD_{50} in rats is 260 ppm [Cincinnati, 1991a]. Cats exposed to 2800 ppm for 30 minutes developed fatal pulmonary edema [Hathaway et al., 1991]. Solutions to 10 percent and 100 percent

furfural instilled in rabbits eyes causes pain in addition to transient swelling and redness of the lids and conjunctiva [Grant et al., 1986]. Chronic dietary exposure to furfural causes liver cirrhosis in rats [Bethesda, 1992]. Dogs exposed at 130 ppm for 6 hours a day for 4 weeks develops liver damage, but dogs exposed at 63 ppm did not [Cincinnati, 1994]. Rabbits exposed to furfural vapours for several hours daily develop liver and kidney lesions as well as changes in their blood profiles [Parmeggiani et al., 1983]. Furfural is mutagenic in at least one bacterial species [Cincinnati, 1991a, http://www.osha.gov/SLTC/healthguidelines/furfural/recognition.html].

Furfural concentrations of 1.9-14 ppm causes headache, itching of the throat, redness and tearing of the eyes in some exposed workers [Cincinnati, 1991[b]; Grant, 1986]. Workers exposed to furfural vapours in a plant with inadequate ventilation report numbness of the tongue and mucous membranes of the mouth, loss of taste sensation, and difficulty in breathing & damage to the eyesight of some individuals has also been reported [Cincinnati, 1991b]. Exposures to high concentrations have produced pulmonary edema [Parmeggiani, 1983]. Chronic skin exposure may produce eczema, allergic skin sensitization, and photosensitization [Sittig, 1991]. Furfural may cause a disulfiram-type reaction, i.e., a worker exposed to furfural, who has consumed alcohol may experience warmth and redness of the fact, a throbbing sensation and pain in the head and neck, difficulty in breathing, nausea, vomiting, sweating, thirst, chest pain, uneasiness, weakness, dizziness, blurred vision, and confusion. This effect may last from 30 minutes to several hours but does not appear to have residual side effects. By analogy with effects seen in animals, furfural may affect the central nervous system, liver, kidneys, blood, and bone marrow of humans; however, these effects have not been reported in exposed workers.

1.4 SOURCES OF HUMAN AND ENVIRONMENTAL EXPOSURE:

Furfural is found in a number of dietary sources. Because of its formation during the thermal decomposition of carbohydrates, furfural is found in numerous processed foods and beverages, including cocoa, coffee, tea, beer, wine, milk products, and bread (Maga, 1979). It is also found in some fruits and vegetables, and it is added as a flavouring agent to some foods. It has also been found in the essential oils of camphor, citronella, sassafras, lavender, and lime (Dunlop and Peters,1953).

Furfural is produced commercially in batch or continuous digesters where pentosans from agricultural residues, including corn cobs, oat hulls, rice hulls, and bagasse, are hydrolysed to pentoses and the pentoses are subsequently cyclodehydrated to Furfural

1.5 HEALTH AND SAFETY IMPACT OF FURFURAL

1.5.1 HEALTH IMPACT

Table 1.6 and fig 1.2 gives the summary of the major type of exposure to furfural and their effect on human health.

1.5.2 SAFETY IMPACT

For safety point of view some standard limits have set as flash point: 60 ^{O}C, Auto ignition temperature is 316 ^{O}C, Lower exposure limit is 2.1 while the Upper Exposure Limit is 19.3. The Oral LD_{50}, Redwing Blackbird is 98.0 mg/kg and the OSHA permissible exposure limit (PEL) is 5 mg/L (TWA) and the skin ACGIH Threshold limit value (TLV) is 2 mg/L (TWA) skin. Above flash point, vapour-air mixtures are explosive within flammable limits noted above. Furfural reacts violently with oxidants, strong acids and bases causing fire and explosion hazards. Sealed containers may rupture when they are heated. It is highly sensitive to static discharge.

Water spray, dry chemical, alcohol foam, or carbon dioxide can be used as a fire extinguishing media. Water spray may be used to keep fire exposed containers cool. Water may be used to flush spills away from exposures and to dilute spills to non-flammable mixtures [http://www.jtbaker.com/msds/englishhtml/f8040.htm].

1.6 LOW COST ADSORBENT

Although Activated carbon, commonly used adsorbent has its own limitations. Because of cost and 10-15% loss in adsorption capacity during regeneration, the overall treatment process becomes costly and is a major constraint in its utilization in developing countries. This has led to search for cheaper carbonaceous substitutes to activated carbon. Recently, bagasse fly ash derived from sugar mills have used as a low cost adsorbent [Sahu et al., 2008; Mall et al., 2005, 2006, 2007; Srivastava et al., 2005, 2006, 2007; Lataye et al., 2006, 2007; Mane et al., 2007] have been investigated for removal of various organics from wastewater. During recent years, various researchers have explored possibilities of utilization of bagasse fly ash as an alternate to activated carbon for the removal of toxic materials [Mall et al., 2005, 2006, 2007; Srivastava et al., 2005, 2006, 2007; Malik et al., 2003; Lataye et al., 2006, 2007; Gupta, 2003].

BFA is a waste material formed during the combustion of bagasse, as a fuel in the boilers of the sugar mills. BFA is also obtained from particulate collection equipment connected to bagasse-fired boilers and emission stacks on the upstream and downstream sides, respectively. About 10 million tonnes of bagasse is produced annually in India. About 90% of this bagasse is used as a fuel in bagasse fired boilers. The production of bagasse fly ash is estimated to be about 3 kg/tonne of sugar produced. With the overall bagasse fly ash collection efficiency of 80% in the dust collection equipment, it is estimated that fly ash availability from the sugar industry

would be of the order of 0.5 million tonnes/year.

The adsorption properties of BFA are highly influenced with the firing practices of bagasse. Several investigators have recently shown interest in the use of bagasse fly ash as an adsorbent. It has been used for the COD removal from sugar mill [Mall et al., 1994], and paper mill effluents [Srivastava et al., 2005a]. BFA has also been used for the adsorptive removal of phenolic compounds [Srivastava et al., 2005b], dyes [Mall et al., 2005a, b], and pyridine [Lataye et al., 2006] from wastewaters.

1.7 OBJECTIVES OF THE PRESENT STUDY

Sahu. et al. (2008 a,b) previously reported adsorptive removal of furfural from aqueous solution by ACC and BFA in batch mode. No work has been found in the open literature on continuous adsorption of furfural bearing wastewater by ACC and BFA. Continues adsorption study of furfural removal is very important from industrial point of view. The present work deals with continuous adsorption of furfural from aqueous solution onto ACC and BFA packed column. The following aims and objectives have been set for the present work.

1. To utilize ACC and BFA as adsorbents for the adsorptive removal of furfural through packed bed and its performance evaluation through prediction of breakthrough curve.
2. To study the effect of various parameters like bed height, initial concentration, flow rate and column diameter on the shape of breakthrough curve and breakthrough time.
3. To utilize various empirical models like Bohart-Adams, Bed depth service time (BDST), Thomas, Yoon-Nelson, Clark and Wolborska models for the prediction of breakthrough curve and to interpret and compare the results so as to obtain the best fit breakthrough model.

Table 1.1: Properties of furfural

Parameter	Details
Name	Furfural
Synonyms	2-furaldehyde, furan, 2-formylfuran etc.,
Chemical formula	$C_5H_4O_2$
Molecular weight	96.09
Physical state	Oily liquid
Appearance	Colourless, when freshly distilled, darkens in contact with air
Odour	Pungent aromatic
Melting Point, °C	-36.5
Boiling point, °C	162
Relative vapour density (air = 1)	3.31
Relative density (water = 1)	1.16
Solubility in water, g/100 ml at 20 °C	8.3
Vapour pressure, kPa at 20 °C	0.144
Flash point, °C	60
Auto-ignition temperature, °C	315
Stability	Stable under ordinary conditions of use and storage

[Source: http://www.osha.gov/SLTC/healthguidelines/furfural/recognition.html]

Table 1.2: Industrial application of furfural

Industry	Uses
Petroleum Refinery	As a solvent in the lube oil extraction unit for removal of napthanic acid and other impurities.
Petrochemicals	As a selective solvent in the production of lubricating oils
Refractories	As a reactive wetting agent in the production of refractory components
Resin manufacture	(a) Production of phenolic resins (b) Production of cashew nutshell polymers
Abrasive materials	As a reactive wetting agent for the resin binder system in the production of abrasive wheels
Solvent recovery	Steam distillation of spent 2-furaldehyde for reuse by industry sectors 1, 2, and 4
Flavouring	Used in very small quantities in synthetic/natural oil blends

Table 1.3: Indian demand of furfural application in various sectors

Sr. No.	User Sector	Consumption in Tonnes		
		1988-89	1992-93	1999-2000
1	Refinery	990	950	950
2	Grinding and Abrasive Wheels	27	33	45
3	Pharmaceuticals	75	120	235
4	Phenolic resins	52	72	120
Total		1104	1175	1350

[Source: www.dsir.nic.in/reports/techreps/tsr048.pdf (Field Investigations)]

Table 1.4 Demand and Supply estimates of furfural in India

Year	Total Demand (Tonnes)	Total Supply (Tonnes)
1988-89	1104	1050
1992-93	1175	5000
1999-2000	1350	5000

[Source: www.dsir.nic.in/reports/techreps/tsr048.pdf (Field Investigations)]

Table1.5: Manufacturers of furfural in India

Name of the company	Raw Material Used
Southern Agrofurane Industries Ltd. Madras (Tamil Nadu)	Bagasse
Oswal Agro Furane Ltd. Ludhiana (Punjab)	Rice husk
Furfur chemicals Ltd. Hyderabad (Andhra Pradesh)	Rice husk

[Source: www.dsir.nic.in/reports/techreps/tsr048.pdf (Field Investigations)]

Table 1.6 Health effect of furfural

Exposure	Effects
Inhalation	Causes irritation to the mucous membranes and upper respiratory tract. Symptoms may include sore throat, labored breathing, and headache. Higher concentrations act on the central nervous system and may cause lung congestion. Inhalation may be fatal.
Ingestion:	Highly toxic. It may cause gastrointestinal disorders, nerve depression and severe headache and may be fatal. Other effects are not well known.
Skin contact	It is highly irritant to skin. It may cause dermatitis and possibly eczema, allergic sensitisation and photosensitisation. It may be absorbed through the skin with possible systemic effects.
Eye contact:	Vapours irritate the eyes, causing tearing, itching, and redness. Splashes may cause severe irritation or eye damage.
Chronic exposure	It can cause numbness of the tongue, loss of sense of taste, headache. Other effects are not well known.
Aggravation of pre-existing conditions	Persons with pre-existing skin disorders or eye problems, or impaired liver, kidney or respiratory function may be more susceptible to the effects of the substance.

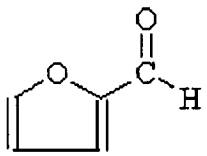

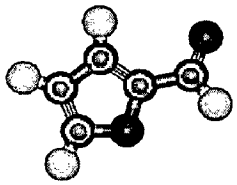

(a) Structural formula of Furfural (b) Cyclic structure of Furfural

Fig 1.1: Structural and Cyclic structure of Furfural

[Source: http://jchemed.chem.wisc.edu/JCEWWW/Features/MonthlyMolecules]

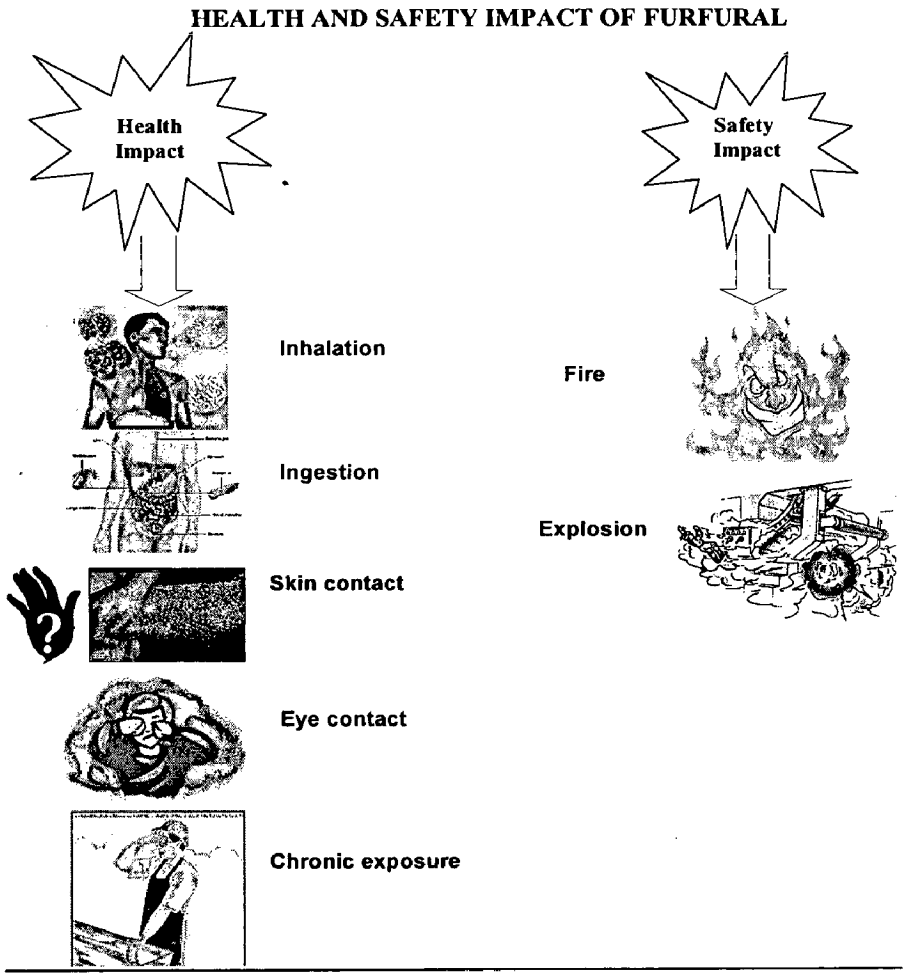

Figure 1.2: Health and safety impact of furfural

Chapter-II

TREATMENT OF FURFURAL: A REVIEW

2.1 GENERAL

The increasing demand in the production of high quality fuels leads the use of various solvents in the process. Furfural is one of popular solvent used in lube extraction unit in petroleum refineries. Besides this it have a wide involvements in some other industries like in manufacturing of phenolic resins, used as a chemical intermediate, weed killer, fungicide and also as a flavoring agent [Othmer et al., 1984]. During these processes furfural gets discharged into the wastewater stream. Sulfite pulping processes used in the pulp and paper industry is one of the sources of furfural contamination [Rivard et al., 1991]. Furfural is highly toxic in nature and its presence in water makes it unusable.

Biological treatments for the degradation of furfural have been used by many researchers, including aerobic and anaerobic processes [Kim et al., 1983; Pitter et al., 1976; Rowe and Tullos, 1980; Kawasaki, 1980; Wang, 1994]. However, these processes are costly and cannot be used by small industries to treat furfural-laden wastewater.

Solvent extraction recovery of furfural from aqueous solutions can be a suitable industrial method with low content of solute. Data on liquid-liquid extraction of furfural have been reported. In an attempt to find suitable solvents for extraction of furfural, liquid-liquid equilibrium data with trichloroethylene, perchloroethylene, 1,2 di-chloroethane, 1,1,1-trichloroethane, and 1,1,2-trichloroethane as solvents were studied at

25 °C. Among the solvents studied, 1,2-dichloroethane and trichloroethylene show the highest selectivity [Coca et al., 1980].

The adsorption process provides an attractive alternative treatment, especially if the adsorbent is cheap and readily available. The polymeric adsorbent XAD-4 and XAD-7 have been used for removal of furfural from pretreated and hydrolyzed plant biomass [Weil et al., 2002]. However, these are expensive and its regeneration and reuse makes it more costly. Consequently, several low cost adsorbents like wood [Poots et al., 1976; Abo-Elela and El-Dib, 1987], coir pith [Namasivayam et al., 2001], coal fly ash [Rao et al., 1978; Gupta et al., 1985; Kumar et al., 2000], bagasse fly ash (BFA) [Mall et al., 1994; Swamy et al., 1997; Swamy et al., 1998; Mall et al., 1998] and coal-fired boiler bottom ash [Mall et al., 1994] have been used for the treatment of a wide variety of wastewaters. Mall et al. [1996] and Bailey et al. [1999] have presented a critical review on the utilisation of low cost adsorbents. Bagasse fly ash has good adsorptive properties and has been used for the removal of COD and colour from sugar mill [Mall et al., 1994] and paper mill effluents [Srivastava et al., 2005]. Various researchers have utilised it for the adsorptive removal of phenolic compounds [Mall et al., 2003; Srivastava et al., 2005], furfural [Lataye et al., 2006] and dyes [Mall et al., 2005, 2006].

2.2 ADSORPTION THROUGH PACKED COLUMN

The continuous flow processes are usually operated in fixed bed adsorption columns. These systems are capable of treating large volumes of wastewater and are widely used for treating domestic and industrial wastewater. They may be operated either

in the upflow columns or downflow column. Continuous counter-current columns are generally not used for wastewater treatment due to operational problems.

The most important criterion in the design of column adsorber is the prediction of the column breakthrough or the shape of the adsorption wave front, which determines the bed length (z) and the operating life span of the bed and regeneration times [Walker and Weatherley,1997]. The factors that affect the column breakthrough include both the operating variables as well as the characteristics of the adsorbate and the adsorbent. Several empirical models like Bed depth service time, Adam-Bohart, Yoon-Nelson, Thomas, Clark and Wolborska models have been used by many investigators for the prediction of breakthrough in packed column adsorption. Various investigators have applied these models for prediction of breakthrough curve for adsorptive removal of organic and inorganic pollutant from wastewater. The summary of these studies have shown in Table 3.2.

Table 2.1 Studies on adsorptive removal of furfural using various types of adsorbents

References	Adsorbent/ Solvent	Adsorbate/ Solute	Operations	Results and discussion
Lucas et al., 2004	Activated carbon from supercritical carbon dioxide	Furfural and ethyl acetate	Continuous adsorption study	Fit of the adsorption isotherms showed that the Langmuir model could correlate the experimental data for ethyl acetate satisfactorily and with more simplicity versus other tested models, whereas, Freundlich isotherm is suitable to fit the adsorption data of furfural on activated carbon
Weil et al., 2005	XAD-4 and XAD-7	Furfural	Continuous adsorption study	Fermentation of the resulting hydrolysates with recombinant E.coli ethanologenic strain K011 confirmed that the concentration of furfural in the polymeric adsorbent treated hydrolysate causes negligible fermentation inhibition. Fermentation of XAD-4 treated hydrolysate with E. coli K011 was nearly as rapid as the control medium with ethanol yields at 90% of theoretical
Coca et al., 1980	Chlorinated hydrocarbons	Furfural	Solvent extraction	Liquid-liquid equilibrium data at 25 0C are reported for five ternary systems containing furfural, water and the chlorinated hydrocarbons trichloroethylene, perchloroethylene, 1,2-dichloroethane, 1,l,1-trlchloroethane, and 1,1,2-trlchloroethane. Among the solvents studied, 1,2-dlchloroethane and trichloroethylene show the highest selectivity.
Agrawal et al., 2005	XAD-4	Furfural	Continuous adsorption study	A study of different column length and different feed flow rates were done, keeping column diameter and concentration of feed nearly constant. For each set of condition breakthrough curve was plotted. A comparison between the breakthrough times determined experimentally and by the determination of length of MTZ was done. Regeneration of column was done using acetone.
Sahu. et al., 2008	Bagasse fly ash and activated carbon	Furfural	Batch adsorption study	Adsorption kinetics was found to follow second order rate expression with initial sorption rate being highest for adsorption on BFA. The Redlich–Peterson isotherm, best represented equilibrium adsorption. Adsorption of phenol on BFA is favourably influenced by increase in the temperature of the operation. This shows that the overall sorption process is controlled by intra-particle diffusion of phenol. The negative value of Gibbs free energy indicates spontaneous adsorption of phenol on BFA

Table 2.2: Studies on the prediction of breakthrough curve by Column adsorption

Author/ Year	Adsorbate	Adsorbents	Empirical Models applied	Parameters and their effect on Breakthrough curve Studied	Remark
Das et al. (1993)	Vermiculite	Lead	-	Flow rate, particle size & initial concentration	Close agreement with predicted performance using the batch isotherm data.
Azquez et al. (2006)	Pinus pinaster bark	Phenol	Lin and Wang	Flow rate & initial concentration	Adsorption of phenol is influenced by the inlet phenol concentration as well as by the flow rate. Both the breakthrough time and the dynamic capacity of the bark decreased when the flow rate was increased. The equivalent length of unused bed (LUB) was determined using the LUB Design Approach. The results showed that the LUB increases by decreasing the flow rate.
Dwivedi et al. (2008)	Activated carbon	Lead	Langmuir and Freundlich adsorption isotherm models.	Flow rate & initial concentration	Adsorption of Pb(II) on GAC followed both Adsorption capacity for 60 mg/l feed concentration of Pb(II) at hydraulic loading rate of 12m3/(hm2) and 0.6m bed height is found to be 2.0132 mg/g, which indicates that practically adsorption capacity of GAC is far less than batch mode results.
Aksu et al. (2004)	Immobilized activated sludge	Phenol	Langmuir, Freundlich, Adams–Bohart, The Wolborska Thomas, Clark & Yoon–Nelson	Initial pH, flow rate & initial concentration	Sorption of phenol is dependent on both the flow rate and the inlet phenol concentration and the breakpoint time and phenol removal yield decrease with increasing flow rate and phenol concentration. Isotherm constants were determined by Freundlich and Langmuir adsorption models. The initial region of breakthrough curve was defined by the Adams–Bohart (or Wolborska) model at all flow rates and inlet phenol concentrations studied while the full description of breakthrough could be accomplished by all other models
Teng et al. (2006)	Activated montmorillonite	Methyl orange dye	Adams–Bohart, and Wolborska	Bed height, flow rate & initial concentration.	It was stated that Empirical models applied, could satisfactorily describe the measured breakthrough curves of acid dye in fixed beds (standard deviation < 5%). The effect of the type of clay (raw, HCl-activated) on the values of N0, kAB, and βa was discussed, and the application potential of acid-activated clay for adsorption removal of acid dye from water was also demonstrated.

Contd....					
Lodeiro et al. (2006)	Protonated Sargassum muticum	Cadmium	BDST Bohart–Adams Yan model The Belter and Chu models Bohart–Adams model	Bed height & flow rate	The maximum metal uptake capacity, determined from the area below adsorbed cadmium concentration versus time curves, was found to remain constant with flow rate and with bed depth (if the quantity of biomass is high enough). The best fit of the breakthrough curves, obtained under different experimental conditions tested, was achieved with the Yan model. The bed depth service time model was used to predict the relationship between service time and bed height, which is essential in column process design. The bed sorption capacity and the sorption rate constant can be calculated from these plots.
Han et al. (2008)	Rice husk	Congo red	BDST Adams–Bohart, Thomas, & Yoon–Nelson	Initial pH, flow rate, initial concentration Bed height	Rice husk as adsorbent can be used to removal CR from solution. BDST model adequately described the adsorption of CR onto rice husk by column mode. The biosorption of CR was dependent on the flow rate, the inlet CR concentration and bed depth.
Aksu et al. (2002)	Immobilized activated sludge & activated carbon	chromium(VI)	Freundlich and Langmuir adsorption models	Initial pH, flow rate, initial concentration	Sorption of chromium (VI) is dependent on the flow rate, the inlet chromium(VI) concentration and time and these parameters affect the saturation capacity of both sorbents directly. Granular activated carbon had a higher adsorption capacity for chromium(VI) (147.1 mg g_1), the experimental results indicated that dried activated sludge has also a considerable potential for the removal of chromium(VI) over a wide range of chromium(VI) concentration (18.9mg/g).
Tsai et al. (1999)	Activated carbons	1,1-dichloro-1-fluoroethane	Langmuir, Freundlich, Dubinin–Radushkevich (D–R.model) & Yoon–Nelson	initial concentration	From the experimental results and data regression analysis, the adsorption isotherm obtained at various temperatures can be well-correlated by the Langmuir, Freundlich, and Dubinin–Radushkevich_D–R.models. The simple two-parameter model _i.e. rate constant, kX, and time required for 50% adsorbate breakthrough, t . of Yoon and Nelson was applied for modeling the breakthrough curves of HCFC-141b vapor through granular activated carbon column.
Medvidovi´c et al. (2006)	Natural zeolite–clinoptilolite	Lead	Mass Transfer Zone (MTZ) Model	Flow rate, particle size & initial concentration	Lead can be removed from aqueous solutions very successfully by means of the column exchange process on natural zeolite–clinoptilolite, with successive service and regeneration cycles. The Bed Volume (BV) at the breakthrough point decreases with the increase of lead concentration in the initial solution, at the same flow. When the flow increases for the solutions of the same lead concentration, the BV at breakthrough points remains nearly the same, but the time it takes to reach the breakthrough point becomes shorter as the flow increases.

Chapter – III

ADSORPTION FUNDAMENTALS AND BREAKTHROGH MODELING

3.1 GENERAL

Adsorption is a surface phenomenon. It is used as a separation process where a species present in a fluid phase is transferred to the solid phase and gets attached to the solid surface, if the concentration of the species in the fluid-solid boundary region is higher than that in the bulk of the fluid [Tien, 1994]. In an adsorption process, molecules or atoms or ions in the fluid phase get concentrated or accumulated on the surface of a solid, where they bond with the solid surface or are held there by weak inter-molecular forces. The accumulated or concentrated species on the surface of solid is called the adsorbate, and the porous solid material is known as an adsorbent. In this chapter, the fundamentals of adsorption onto adsorbents are presented: These fundamentals may be used for the adsorption of furfural and its derivatives onto adsorbents.

3.2 ADSORPTION DIFFUSION STUDY

The mathematical treatment of Boyd et al. [1947] and Reichenberg [1953] to distinguish between the particle, and film diffusion and mass action-controlled mechanism of exchange have laid the foundations of sorption/ion-exchange kinetics. In adsorption systems, the mass transfer of solute or adsorbate onto and within the adsorbent particle directly affects the adsorption rate. It is not only important to study the rate at which the solute is removed from aqueous solution in order to apply

adsorption by solid particles to industrial uses but also it is necessary to identify the step that governs the overall removal rate in the adsorption process in order to interpret the experimental data. There are essentially four steps in the adsorption of a solute from the bulk liquid solution by an adsorbent.

1. Transport of solute from the bulk of the solution to the external film surrounding the adsorbent particle(assumed to be very fast in agitated vessels)
2. Diffusion of the adsorbate from across the external liquid film to the external surface of the adsorbent particle (film diffusion; the resistance could be neglected for properly mixed/agitated vessels)
3. Diffusion of the adsorbate from the poremouth through the pores to the immediate vicinity of the internal adsorbent surface (pore, surface and molecular diffusion)
4. Adsorption of the adsorbate onto the interior surface of the adsorbent.

All these processes play a role in the overall sorption of the solute from the bulk liquid solution to the internal surface of an adsorbent. In a rapidly stirred, well mixed batch adsorption, mass transport from the bulk solution to the external surface of the adsorbent is usually rapid. Therefore, the transport resistance of the adsorbate from the bulk of the solution to the exterior film surrounding the adsorbent may be small and can be neglected. In addition, the adsorption of adsorbate at surface sites (step 4) is usually very rapid, and thus offers negligible resistance in comparison to other steps, i.e. steps 2 and 3. Thus, these processes usually are not considered to be the rate-limiting steps in the sorption process. In most cases, steps (2) and (3) may control the sorption phenomena. For the remaining two steps in the overall adsorbate transport, three

distinct cases may occur:

Case I: external transport resistance > internal transport resistance

Case II: external transport resistance < internal transport resistance

Case III: external transport resistance ≈ internal transport resistance

In cases I and II, the overall rate is governed by the film diffusion and diffusion in the pores, respectively. In case III, the transport of solute to the boundary may not be possible at a significant rate, thereby, leading to the formation of a liquid film with a concentration gradient surrounding the adsorbent particles.

Usually, external transport is the rate-limiting step in systems which have (a) poor phase mixing, (b) dilute concentration of adsorbate, (c) small particle size, and (d) high affinity of the adsorbate for the adsorbent. In contrast, the intra-particle step limits the overall sorption for systems that have (a) a high concentration of adsorbate, (b) a good phase mixing, (c) large particle size of the adsorbents, and (d) low affinity of the adsorbate for the adsorbent.

3.3 ADSORPTION KINETIC STUDY

In order to investigate the adsorption processes, various kinetic models are used to describe the time-course of adsorption of a species onto an adsorbent. The kinetic models include pseudo-first-order, pseudo-second-order, rate expressions when the diffusional mass transfer resistances (external to solid, i.e. in the fluid phase, and internal-pore and surface diffusion) are considered to be negligible. The mass transfer based models include intra-particle diffusion model, Elovich model, Bangham model and modified Freundlich models. Table 3.1 listed these models with their equations.

3.4 ADSORPTION EQUILIBRIUM STUDY

The successful representation of the dynamic adsorption of solute from a solution onto an adsorbent depends upon the equilibrium between the two phases. Adsorption equilibrium is established when the amount of adsorbate adsorbed on the solid surface of adsorbent is equal to the amount desorbed. At its equilibrium condition the amount of solute adsorbed on the solid adsorbent surface and the solution concentration remain constant. The relationship between the amount of adsorbate adsorbed and the adsorbate concentration remaining in solution is described by an isotherm. The adsorption isotherm can be depicted by plotting solid phase concentration against liquid phase concentration graphically. To optimize the design of an adsorption system for the adsorption of adsorbates, it is important to establish the most appropriate correlation for the equilibrium curves. Equilibrium isotherms are measured to determine the capacity of the adsorbent for the adsorbate. Various isotherm equations like those of Langmuir, Freundlich, Temkin and Redlich-Peterson (R-P) have been used by various researchers to describe the equilibrium characteristics of adsorption from liquid solutions. Table 3.2 summarize some important isotherms used with their equations.

3.5 ADSORPTION PRACTICES

Adsorption systems are run either on batch or on continuous basis. Following text gives a brief account of both types of systems as in practice.

3.5.1 Batch Adsorption Systems

In a batch adsorption process, the adsorbent is mixed with the solution to be treated in a suitable reaction vessel for the stipulated period of time, until the concentration of adsorbate in solution reaches an equilibrium value. Agitation is

generally provided to ensure proper contact of the two phases. After the equilibrium is attained, the adsorbent is separated from the liquid through any of the methods available like filtration, centrifuging or settling. The adsorbent can be regenerated and reused depending upon the case.

3.5.2 Continuous Adsorption Systems

The continuous flow processes are usually operated in fixed bed adsorption columns. These systems are capable of treating large volumes of wastewater and are widely used for treating domestic and industrial wastewater. They may be operated either in the upflow columns or downflow column. Continuous counter-current columns are generally not used for wastewater treatment due to operational problems.

Fluidized beds have higher operating costs. So these are not common in use. Wastewater usually contains several compounds, which have different properties and which are adsorbed at different rates. Biological reactions occurring in the column may also function as filter bed retaining solids entering with feed. As a result of these and other complicating factors, laboratory or pilot plant studies on specific wastewater to be treated should be carried out. The variables to be examined include type of adsorbent and its particle size, liquid feed rate, solute concentration in feed, height of adsorbent bed and column diameter. The most important criterion in the design of column adsorber is the prediction of the column breakthrough or the shape of the adsorption wave front, which determines the bed length (z) and the operating life span of the bed and regeneration times [Walker and Weatherley,1997]. The factors that affect the column breakthrough include both the operating variables as well as the characteristics of the adsorbate and the adsorbent.

3.6 BEHAVIOR OF CARBON ADSORPTION COLUMNS

Adsorption Columns behave in much some way as ion exchange columns during operation. When wastewater is introduced at the top or from bottom of a clean bed of activated carbon, most solute removal initially occurs in a rather narrow band at the top of the column, referred to as the adsorption zone. As operation continues, the upper layers of carbon become saturated with solute and the adsorption zone progresses downward through the bed. Eventually, the adsorption zone reaches the bottom of the column, and the solute concentration in the effluent begins to increase. A plot of effluent solute concentration vs. time usually yields as S-shaped curve, referred to as a breakthrough curve. The formation and movement of the adsorption zone and the resulting breakthrough curve are shown in Figure 3.1. The point where the effluent solute concentration reaches 95% of its influent value is usually called the point of column exhaustion. The formation and movement of the adsorption zone has been described mathematically by Michaels [1952].

The time required for the exchange zone to move the length of its own height down the column once it has become established is

$$t_z = \frac{V_s}{Q_w} \qquad (3.1)$$

Where, V_s is the total volume of wastewater treated between breakthrough and exhaustion (m^3) and Q_w is the wastewater flow rate (m^3/sec).

The time required for the exchange zone to become established and move completely out of the bed is

$$t_E = \frac{V_E}{Q_w} \qquad (3.2)$$

Where, V_E is total volume of wastewater treated to the point of exhaustion (m^3).

The rate at which the adsorption zone is moving down through the bed is

$$Uz = \frac{h_z}{t_z} = \frac{h}{t_E - t_F} \qquad (3.3)$$

Where, h_z is the height of exchange zone (m), h is the total column height (m) and t_F is the time required for the exchange zone to initially form (sec).

Rearranging equation 3.3 provides an expression for the height of the exchange zone, an important design parameter:

$$h_z = \frac{h(t_z)}{t_E - t_F} \qquad (3.4)$$

All the terms in the equation 3.2 to 3.4, with the expression of t_F, can be easily evaluated by conducting a laboratory column study. The value of t_F can not be measured directly but the limits for t_F can be established by further analysis of the adsorption zone.

If the carbon within the adsorption zone were completely exhausted, it would contain an amount of solute equal to

$$S_{max} = C_0(V_E - V_B) \qquad (3.5)$$

Where C_0 = the initial solute concentration (mg/m^3) and $(V_E - V_B)$ is the volume of wastewater treated between breakthrough and exhaustion (m^3).

However, only a fraction of carbon within the adsorption zone contains solute. The amount of solute that has been removed by the adsorption zone from breakthrough to exhaustion is the area left to the curve in figure 3.1.

This area represents an amount of solute, S_z, such that

$$S_z = \int_{V_B}^{V_E} (C_0 - C)dV \qquad (3.6)$$

At breakthrough the fraction of carbon present in the adsorption zone still processing ability to remove solute is

$$F = \frac{S_z}{S_{\max}} = \frac{\int_{V_B}^{V_E} (C_0 - C)dV}{C_0(V_E - V_B)} \qquad (3.7)$$

$$F = \int_0^1 (1 - \frac{C}{C_0}) d \frac{(V - V_B)}{(V_E - V_B)} \qquad (3.8)$$

If the adsorption zone is essentially saturated at breakthrough, the value of F will be very close to zero and the time required for the zone to form initially (t_F) will be approximately the same as the time required for the zone to move down a distance equal to its own height. If the adsorption zone is practically free of solute at the breakpoint, the time required for the zone formation is very short. If the concentration front is characterized by a typical S-shaped curve, F is approximately 0.5.

The time for zone formation can be then be written as a function of zone velocity;

$$t_F = (1 - F)t_z \qquad (3.9)$$

Substituting equation into equation yields a ratio of zone height to total column height;

$$\frac{h_z}{h} = \frac{t_z}{t_E - (1 - F)t_z} \qquad (3.10)$$

If all of the column were completely saturated, the total amount of solute adsorbed would be

$$S_T = \rho(h)\left[\frac{x}{m}\right]_s A_{cs} \qquad (3.11)$$

Where, ρ is the apparent packed density of carbon in the bed (mg/m^3), h is the total height of carbon in bed (m), $\left[\frac{x}{m}\right]_s$ is the amount of solute adsorbed per unit weight of carbon at saturation (mg/mg) and A_{cs} is the cross-sectional area of column m^2.

At the breakpoint, an adsorption column will not be completely saturated but will be composed of the partially exhausted adsorption zone and the totally exhausted material located above the adsorption zone. The height of the exhausted zone is $(h-h_z)$, and the total amount of solute adsorbed in the column is

$$S_B = \left[\frac{x}{m}\right]_s \rho[(h-h_z)+Fh_z]A_{cs} \qquad (3.12)$$

The percentage of the total column saturated at breakthrough is

$$\%\ \text{saturation} = \frac{\left[\frac{x}{m}\right]_s \rho[(h-h_z)+Fh_z]A_{cs}}{\rho(h)\left[\frac{x}{m}\right]_s A_{cs}} \qquad (3.13)$$

$$\%\ \text{saturation} = \frac{h+(F-1)h_z}{h}\times 100 \qquad (3.14)$$

The shape of breakthrough curve depends on the nature of the wastewater being treated. If there is only one adsorbable component in the wastewater, the adsorption zone will be short and the breakthrough curve will be steep like curve (a) in figure [Fornwalt and Hutchins, 1966a]. If there is a mixture of components having different adsorbabilities, the adsorption zone will be deep and the breakthrough curve will be gradual like curve (b) in Figure 3.2. According to Fornwalt and Hutchins (1966a), if the breakthrough curve is steep such that breakthrough occurs near the point of column exhaustion (curve a) single column operation is feasible. However, if the breakthrough

concentration is reached before the column is fully exhausted (curve b), a multiple column installation is preferable.

3.7 MODELS FOR PREDICTION OF BREAKTHROUGH TIME

The most important criterion in the design of column adsorber is the prediction of the column breakthrough or the shape of the adsorption wave front, which determines the bed depth (z) and the operating life span of the bed and regeneration times [Walker and Weatherley, 1997]. The factors that affect the column breakthrough include both the operating variables as well as the characteristics of the adsorbate and the adsorbent. Several models have been used for the prediction of breakthrough. Some of these are discussed below:

3.7.1 Bed depth service time (BDST) model

BDST model is based on the assumption that the rate of adsorption is controlled by the surface reaction between the adsorbate and the residual capacity of the adsorbent. The Bohart-Adams model is used for the description of the initial part of the breakthrough curve which relates C/Co with t for a continuous flow adsorber column [Bohart and Adams, 1920]. This equation is given as

$$\ln\left(\frac{C_0}{C}-1\right)=\ln\left[\exp\left(kN_0\frac{Z}{U}\right)-1\right]-kC_0t \qquad (3.15)$$

Where, C_0 is the initial concentration of the solute (mg/L), C is the desired concentration of the solute at time t (mg/L), k is the adsorption rate constant for the column (L/min mg), Z is the depth of the bed (cm), N_0 is the adsorptive capacity of adsorbent (mg/L) and U is the linear flow velocity of the feed to the bed (cm/min). Hutchins [1973] linearized Eq. (1) as follows:

$$t = \frac{N_0}{C_0 U_0} Z - \frac{1}{kC_0} \ln\left(\frac{C_0}{C} - 1\right) \qquad (3.16)$$

This equation predicts linear BDST plots between t and Z. The adsorptive capacity of the system N_0 can be evaluated from the slope of the plot whereas the rate constant k can be calculated from the intercept, I.

Where, $$I = -\left(\frac{1}{kC_0}\right) \ln\left(\frac{C_0}{C} - 1\right) \qquad (3.17)$$

The value of N_0 can also be calculated in a more convenient way as follows. At 50% breakthrough, C_0/C = 2 and $t = t_{0.5}$, and therefore, the final term in the Eq. (3.16) becomes zero, yielding the following relationship:

$$t_{0.5} = \frac{N_0}{C_0 U} Z \qquad (3.18)$$

Thus a plot of time at 50% breakthrough, $t_{0.5}$ against Z should be a straight line passing through the origin, allowing N_0 to be calculated.

3.7.2. Thomas model

Thomas model [Thomas, 1944] assumes negligible axial dispersion in the bed, uses Langmuir isotherm for equilibrium and second-order reversible reaction kinetics. The model also assumes a constant separation factor but is applicable to either favorable or unfavorable adsorption conditions. The primary weakness of the model is that its derivation is based on the second order reaction kinetics. Adsorption is usually not limited by chemical reaction kinetics but is often controlled by interphase mass transfer. Therefore, this model is suitable for adsorption processes where the external and internal diffusion limitations are absent [Aksu and Gönen, 2004]. The model

application can lead to some error in adsorption processes where first-order reaction kinetics is followed [Rao and Viraraghavan, 2002]. The Thomas model is given as:

$$\frac{C}{C_0} = \frac{1}{1+\exp\left[k_T\left(Q_0 m_C - C_0 V_{eff}\right)/Q\right]} \qquad (3.19)$$

Where, k_T is the Thomas rate constant (L/min mg), Q_0 the maximum solid-phase concentration of the solute (mg/g), m_C the mass of the adsorbent in the column (g), V_{eff} the throughput volume (L), and Q is the volumetric flow rate (L/min). The linearized form of the Thomas model is given as:

$$\ln\left(\frac{C_0}{C}-1\right) = \frac{k_T Q_0 m}{Q} - \frac{k_T C_0}{Q} V_{eff} \qquad (3.20)$$

The kinetic coefficient k_T and the adsorption capacity of the bed Q_0 can be determined from the intercept and the slope of the plot of $\ln[(C_0/C)-1]$ against t at a given flow rate.

3.7.3 Yoon and Nelson model

Yoon and Nelson [1984] have developed a relatively simple model addressing the adsorption and breakthrough of adsorbate vapors or gases with respect to activated charcoal. This model is based on the assumption that the rate of decrease in the probability of adsorption for each adsorbate molecule is proportional to the probability of the adsorbate adsorption and the adsorbate breakthrough on the adsorbent [Aksu and Gönen, 2004]. The Yoon and Nelson equation for the 50% breakthrough concentration from a fixed bed of adsorbents is given as:

$$\ln\left(\frac{C}{C_0 - C}\right) = k_{YN} t - t_{0.5} k_{YN} \qquad (3.21)$$

Where, k_{YN} is the Yoon-Nelson rate constant (min^{-1}). k_{YN} and $t_{0.5}$ may be obtained from the slope and the intercept of the linear plot of $\ln[C/(C_0 - C)]$ versus t.

3.7.4. Clark model

Clark [1987] used the mass transfer coefficient concept in combination with the Freundlich isotherm to define a new relation for the breakthrough curve:

$$\frac{C}{C_0} = \left(\frac{1}{1 + Ae^{-rt}}\right)^{1/n-1} \tag{3.22}$$

with

$$A = \left(\frac{C_0^{n-1}}{C_b^{n-1}} - 1\right) e^{rt_b} \tag{3.23}$$

and

$$r = \frac{\beta}{U} v_m (n-1) \tag{3.24}$$

Where, n is the Freundlich constant, C_b is the concentration of the solute at breakthrough time t_b (mg/L) and v_m is the migration velocity of the concentration front in the bed (cm/min). v_m can be determined from the following relationship:

$$v_m = \frac{UC_0}{N_0 + C_0} \tag{3.25}$$

Eq. (3.22) can be rearranged to the following linear form:

$$\ln\left[\left(\frac{C_0}{C}\right)^{n-1} - 1\right] = -rt + \ln A \tag{3.26}$$

For a particular adsorption process on a fixed bed and a chosen treatment objective, values of A and r can be determined by using the above equation, enabling the prediction of the breakthrough curve.

3.7.5. The Wolborska model:

Wolborska [1989] found the following relationship describing the concentration distribution in the bed for the low concentration region of the breakthrough curve:

$$\ln\frac{C}{C_0}=\frac{\beta C_0}{N_0}t-\frac{\beta Z}{U} \qquad (3.27)$$

Where, β is the kinetic coefficient of the external mass transfer (min^{-1}) and other symbols have usual meanings. β and N_0 can be determined from a plot of $\ln(C/C_0)$ against t at a given bed height and flow rate.

3.8 Error Analysis:

The dynamic behavior of the column can be predicted by using the Bohart-Adams, Thomas, Yoon-Nelson, Clark and Wolborska models. Linear regression coefficients (R^2) show the adequacy of the fit between experimental data and the linearized forms the equations, while the estimation of error between the experimental and predicted values of C/Co can be calculated by the Marquardt's percent standard deviation (MPSD) [Marquadt, 1963].

$$\text{MPSD} = 100\sqrt{\frac{1}{N-P}\sum_{i=1}^{n}\left(\frac{(C/C_0)_{\exp}-(C/C_0)_{theo}}{(C/C_0)_{\exp}}\right)_i^2} \qquad (3.28)$$

Where, N is the number of data points and P is the number of parameters (or the degrees of freedom of the system. Also, the percent deviation between the experimental and theoretical time for the breakthrough can be calculated using Eq. (3.29).

$$\varepsilon = 100\left(\frac{t_{b,\exp}-t_{b,cal}}{t_{b,\exp}}\right) \qquad (3.29)$$

Table 3.1 Adsorption Kinetic Models

Sr. No.	Kinetic Model	Governing Equations
1	Pseudo-First-Order Model [Fogler, 1998]	$\frac{X_A}{X_{Ae}} = 1 - \exp\left[k_A C_S + \frac{k_A}{K_S}\right]t$
2	Pseudo-Second-Order Model [Ho and Mckay, 1998, 1999, 2000]	$\frac{dq}{dt} = k_S(q_e - q_t)^2$
3	Intra-particle Diffusion [Ho and Mckay, 1998, 1999, 2000]	$\frac{dq}{dt} = k_S(q_e - q_t)^2$
4	Elovich Model [Cheung et al. 2000, Onal, 2006]	$\frac{dq_t}{dt} = \alpha e^{-\beta q_t}$
5	Bangham's Equation [Aharoni et al., 1979]	$\log\log\left(\frac{C_0}{C_0 - q_t m}\right) = \log\left(\frac{k_{0B} m}{2.303V}\right) + \alpha\log(t)$
6	Modified Freundlich Equation [Kuo and Lotse, 1973]	$q_t = kC_0 t^{1/m}$

Table 3.2: Isotherms and their governing equation

Sr. No.	Isotherm	Governing Equations
1	Langmuir, [1918]	$q_e = \frac{q_m K_L C_e}{1 + K_L C_e}$
2	Freundlich, [1906]	$q_e = K_F C_e^{1/n}$
3	Redlich–Peterson, [1959]	$q_e = \frac{K_R C_e}{1 + a_R C_e^{\beta}}$
4	Temkin, [1940]	$q_e = \frac{RT}{b}\ln(K_T C_e)$
5	Toth, [1971]	$q_e = \frac{q_e^{\infty} C_e}{\left[1/K_{th} + C_e^{Th}\right]^{1/Th}}$
6	Radke and Prausnitz, [1972]	$q_e = \frac{K_{RP} k_{rp} C_e}{1 + K_{RP} C_e^{P}}$

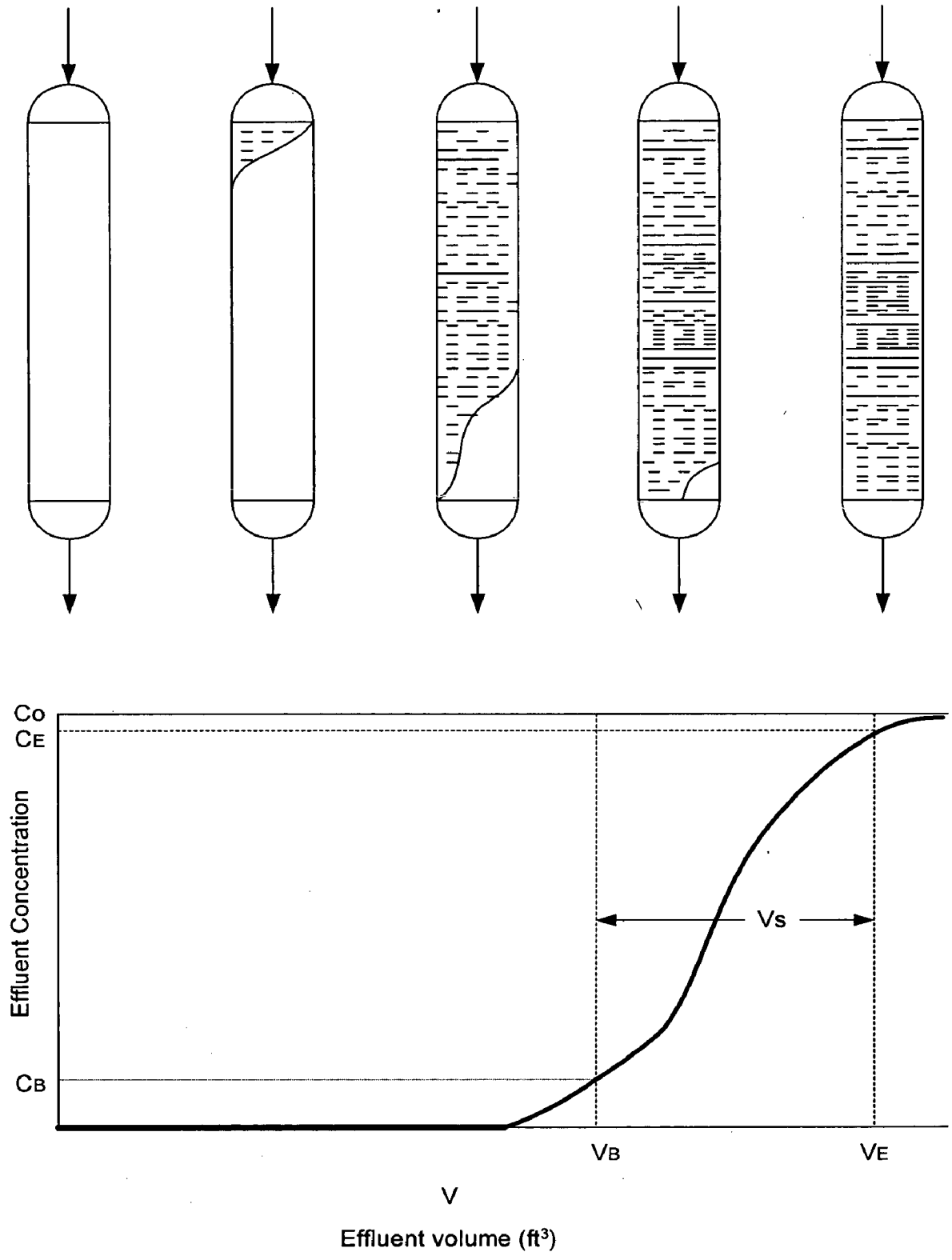

Figure 3.1: Idealized Breakthrough Curve for Carbon adsorption column

[Source: Larry D. Benefield, "Process Chemistry for water and wastewater treatment"]

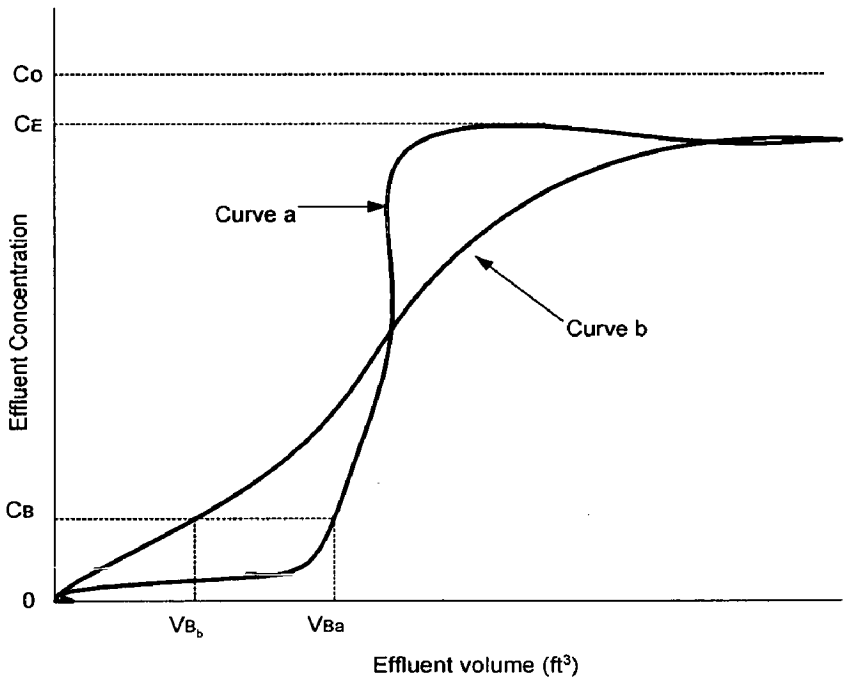

Figure 3.2: Typical Adsorption breakthrough curves

[Source: Larry D. Benefield, "Process Chemistry for water and wastewater treatment"]

CHAPTER – IV

EXPERIMENTAL PROGRAMME

4.1 GENERAL

In the present study, activated carbon commercial grade (ACC) and bagasse fly ash (BFA) have been utilized for the treatment of furfural-laden aqueous solution through packed column. Experimental details of the study have been presented in this chapter. These details include characterization of adsorbents and continuous adsorption studies.

4.2 CHARACTERIZATION OF ADSORBENTS

Coconut-based ACC was supplied by ZeoTech Adsorbents Pvt. Ltd., New Delhi, India and bagasse fly ash (BFA) was obtained from Deoband sugar mill, U.P., India. Detailed physico-chemical characteristics of the ACC and BFA have already been presented by Sahu et al. [2008 a,b].

4.3 ADSORBATE

Furfural supplied by S D Fine Chemicals, Mumbai (India) was used as adsorbate. Stock aqueous solution of 1000 mg/L was prepared by dissolving accurate quantity of furfural in distilled water. Further, the solutions of required concentration were prepared by using same stock solution.

4.4 ANALYTICAL MEASUREMENT

The determination of the concentration of furfural was done by finding out the absorbance characteristic wavelength using UV/VIS spectrophotometer (HACH, DR/5000). A standard solution of known concentration of furfural was taken and the absorbance was determined at different wavelengths to obtain a plot of absorbance versus wavelength. The wavelength corresponding to maximum absorbance (λ_{max}) was determined from this plot. The λ_{max} for furfural was found to be 277 nm. Calibration curve was plotted between the absorbance and the concentration of furfural solution.

The linearity of calibration curve [Fig. 4.1] indicates the applicability of the Lambert-Beer's Law.

4.5 COLUMN ADSORPTION EXPERIMENTS

To study the effect of various parameters like Influent furfural concentration (C_0), flow rate (Q), bed height (Z) and bed diameter (D) on the adsorptive removal of furfural by Column packed with ACC and BFA were conducted at 303 K. The experiments were carried out in three plexiglass columns of inside diameter, D=2, 2.54 and 4 cm; and 90 cm length. The columns were provided with a feed port at the bottom centre of the column. The lower portion of the column was filled with the pieces of 0.4-0.5 cm diameter glass beads up to a height of 1.5 cm and this portion was used for the uniform distribution of the solution across the whole cross section of the column and to dampen the fluctuating flow phenomena induced by the peristaltic pump. The portion was attached to the main column through two flanges with O-ring rubber seals and a sintered metal disc in between.

The column was packed with activated carbon up to different bed height, viz., 15, 30, 45 and 60 cm from the bottom and was loaded with aqueous solution of phenol using a peristaltic pump (Miclins PP20). The solution flowed upwards. Sampling ports were provided at 15, 30, 45 and 60 cm from the bottom. Samples were withdrawn from different ports at different time intervals. The influent concentration of furfural in aqueous solution for all experimental runs was taken within the range Co=50-200 mg/L. pH of feed was kept at its natural value ($pH=6.5$) with out any alteration. Flow rate of feed was varied between 0.02 to 0.04 L/min.

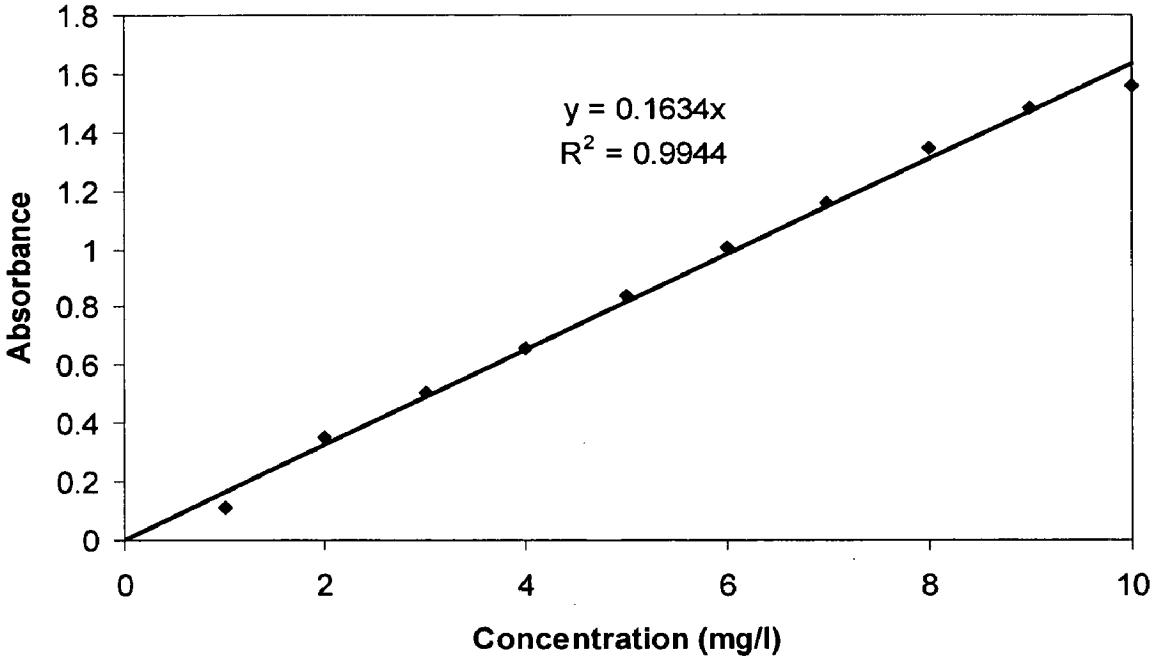

Fig. 4.1: Calibration graph upto furfural concentration 10 mg/L for determination of furfural concentration

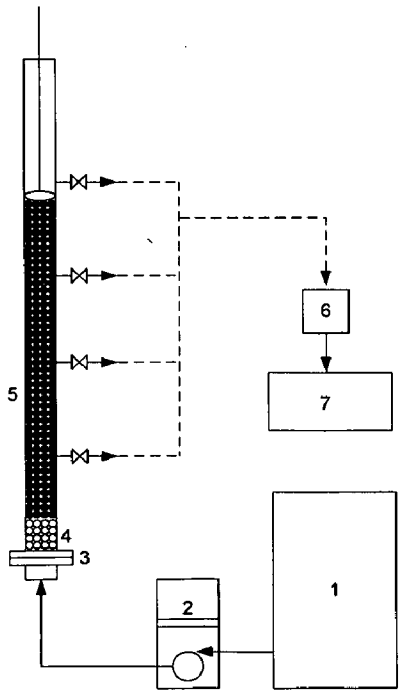

Fig. 4.2: Schematic diagram of experimental set up: (1) Reservoir tank with aqueous solution of furfural, (2) peristaltic pump, (3) supporting flange, (4) glass beads, (5) column,(6) filter media ,(7) effluent storage.

CHAPTER – V

RESULTS AND DISCUSSION

5.1 GENERAL

The detailed discussion on the results of the experiments conducted for the removal of furfural by bagasse fly ash (BFA) and activated carbon commercial grade (ACC) is given in this chapter. These results include:

- Prediction of breakthrough curve in adsorptive removal of furfural through ACC and BFA packed column.
- Effect of various design parameters namely Bed height (Z), feed concentration (C_o), flow rate (Q) and column diameter (D) on the breakthrough curve.
- Application of empirical models to experimental data and calculation of various constants related to models.
- Comparison of ACC and BFA performance for furfural removal through packed column.

5.2 CONTINIOUS ADSORPTION STUDY THROUGH ACC PACKED COULUMN

In order to study the removal of furfural through ACC packed column and for prediction of breakthrough curve, the continuous operations were performed. Operational parameters such Z, C_o, Q and D are important in column design. The effects of these parameters on the adsorption capacity of ACC were studied for the furfural uptake.

5.2.1 Effect of bed height (Z)

The breakthrough curves were examined at different Z and the results are shown in Fig. 5.1 by data points. Higher uptake of furfural was observed at highest Z. This was due to the increase in the number of binding sites owing to increase in adsorption surface area of the adsorbent [Rao et al., 2002]. As the value of Z increased, furfural had sufficient time to diffuse into the whole mass of the ACC that resulted in an increase in t_b. The slope of breakthrough curve decreased with an increase in Z due to the broadening of mass transfer zone.

5.2.2 Effect of feed concentration (C_o)

To investigate the effect of C_o on the adsorption of furfural into ACC, Z, Q and D values were kept constant at 60 cm, 0.02 L/min and 2.54 cm, respectively, whereas the value of C_o was changed from 50 to 200 mg/L. Results are presented in Fig. 5.2 by data points. It was found that the value of t_b decreased with an increase in C_o. The larger the C_o, the steeper the slope of the breakthrough curve and smaller the t_b. At low C_o, breakthrough curves were dispersed and breakthrough occurred slower. As the value of C_o increased, sharper breakthrough curves were obtained. This can be explained by the fact that more adsorption sites are being covered with increase in C_o. These results demonstrated that the change of concentration gradient affected the saturation rate and t_b. As the C_o increases, furfural loading rate increases, so does the driving force or mass transfer, which results in a decrease in the adsorption zone length [Goel et al., 2005].

5.2.3 Effect of Flow rate (Q)

The breakthrough curves at various Q values are shown in Fig. 5.3 It is seen from this figure that the breakthrough generally occurred faster with higher Q value. Time required for reaching saturation increased significantly with a decrease in the value of Q. Obviously, the ACC particles saturated early at value of Q. This is because the time required to reach an equilibrium state between ACC particles and furfural solutions is much longer (about 6 h) [Sahu et al., 2008 a]. Therefore, an increase in the Q causes a shorter retention time, which causes a negative effect on the mass transfer efficiency of the adsorbate. At higher value of Q, the rate of mass transfer tends to increase. The amount of furfural adsorbed onto the unit bed height (mass transfer zone) increased with increasing Q leading to faster saturation at a higher value of Q [Ko et al., 2000].

5.2.4 Effect of column diameter (D)

Fig. 5.4 shows the breakthrough curves for the adsorption of furfural in columns of different D when Z, C_o and Q values were kept constant at 60 cm, 100 mg/L and 0.02 L/min, respectively. It is illustrated in figure that the value of t_b increased with an increase in D. For a lower value of D, the bed is better packed so that the control of flow distribution is easier. Sharper profiles were obtained with thin packed beds having a D value of 2 and 2.54 cm. A shallower breakthrough curve and a longer t_b is obtained with wider bed (D=4 cm) which may be due the channeling of the furfural [Srivastava et al., 2008].

5.2.5 Empty bed contact time and adsorbent usage rate

Empty bed contact time (EBCT) is an important parameter in the design of adsorption columns. It affects the shape of the breakthrough curve and breakthrough volume (V_b). This is determined by the following equation:

$$EBCT = \frac{V_C}{Q} = \frac{A_C Z}{Q} \qquad (5.1)$$

The performance of a fixed-bed can be further evaluated in terms of the adsorbent usage rate (U_r) defined as the weight of adsorbent saturated per litre of solution treated, as follows [Srivastava et al., 2008]:

$$U_r = \frac{m_C}{V_b} = \frac{V_C \rho}{V_C N_b} = \frac{\rho}{N_b} \qquad (5.2)$$

Choosing 10% breakthrough point as the treatment objective, the values of EBCT and U_r were determined using the data from the breakthrough curves obtained at various Z, Q and D [Table 5.1]. From these data, it can be seen that the value of U_r tends to decrease with an increase in EBCT.

5.2.6 Application of Bed depth service time Model

Fig. 5.5 shows the application of BDST model for the removal of furfural on a fixed bed of ACC at 10% and 50% breakthrough for a flow rate of 0.02 L/min. A 50% breakthrough curve between t and Z must result in a straight line passing through the origin, however, the straight line does not pass through the origin. The failure of $t_{0.5}$ versus Z curve passing through the origin indicates that the adsorption of furfural onto ACC occurs through complex mechanism, and more than one rate-limiting step are involved in the adsorption process [Sharma et al., 1995; Zulfadhly et al.,2001]. Adsorption capacity (N_0) as calculated from the slope of 50% plot was 7657 mg/L.

After applying Eq. (3.16) to the experimental data at the 10% breakthrough point, a linear relationship is found when the time for 10% breakthrough ($t_{0.1}$) was plotted against bed height, Z, (Fig. 5.5). N_0 and k as calculated from the slope and the intercept of this plot are found to be 4959.5 mg/L and 9.133 x 10^{-5} L/mg min, respectively. N_0 values predicted by 10% breakthrough plot shows deviation of 35.22% as compared to the value predicted by 50% breakthrough plot.

5.2.7 Application of Thomas Model

Thomas model was applied to the data at C/Co ratios higher than 0.08 and lower than 0.99 with respect to bed height and flow rate. A linear plot of $\ln[(C_0/C)-1]$ against V_{eff} enabled the determination of kinetic coefficient k_T and the adsorption capacity of the bed q_0 according to Eq. (3.20). Fig. 5.6, 5.7, 5.8, 5.9 shows the experimental and theoretical breakthrough curves obtained at different bed heights, initial concentration, flow rates and column diameter for the Thomas model. Values of R^2 were found to be > 0.8978 (Table 5.2). k_T and q_0 values are shown in Table 5.2. It can be observed from the Table 5.2 that the values of q_0 generally increased with increase in the value of Z, C_o and D, however, its value decreased with an increase in the value of Q. Table 3 shows that the values of ε are higher at lower value of Z and D, thus, this model gives poorer prediction of breakthrough point at these conditions.

5.2.8 Application of Yoon-Nelson Model

The values of k_{YN} and $t_{0.5}$ were determined from $\ln[C/(C_0-C)]$ versus t at variable operating conditions. These values are listed in Table 5.3. Fig. 5.10, 5.11, 5.12,

5.13 shows the experimental and theoretical breakthrough curves obtained at different bed heights, initial concentration, flow rates and column diameter for the Yoon and Nelson model. The data in Table 5.3 indicate that the $t_{0.5}$ values as predicted from the Yoon and Nelson model matched very well to those predicted from experimental results.

5.2.9 Application of Clark Model

Freundlich constant n = 3.5714 [Sahu et al., 2008 a] has been used in the Clark model to calculate the model parameters for the adsorption of furfural on ACC column. Values of r and A in the Clark equation were determined from the slope and intercept of $\ln\left[(C_0/C)^{n-1}-1\right]$ versus t plot according to Eq. (5). Fig. 5.14, 5.15, 5.16, 5.17 shows the experimental and theoretical breakthrough curves obtained at different bed heights, initial concentration, flow rates and column diameter for the Clark model. Table 5.4 shows the values obtained alongwith the correlation coefficient and MPSD. This model predicted the adsorption breakthrough well for C/Co > 1.5 with respect to all parameters. Below this level, this model could not be predicted the experimental data points. It appears that the simulation of the whole breakthrough curve is impossible using Clark model. In our previous study [Sahu et al., 2008 a], it was found that the Langmuir model better represented the isotherm data as compared to Freundlich isotherm. Since, this model uses the Freundlich constant n as one of the input parameters which did not best represented the batch isotherm data, therefore, Clark model is not able to represent the breakthrough curve properly.

5.2.10 Application of Bohart Adams and Wolborska Model.

For determination of the fit of the Wolborska model, Eq. (3.27) was applied to the experimental data for varying operating parameters. A linear relationship between $\ln(C/C_0)$ and t was obtained for the relative concentration region up to 50% breakthrough. The kinetic coefficients of mass transfer as well as the bed capacity (N_0) were determined by the application of Bohart-Adams model. Fig. 5.18, 5.19, 5.20, 5.21 shows the experimental and theoretical breakthrough curves obtained at different bed heights, initial concentration, flow rates and column diameter for the Bohart adams and Wolborska model. Table 5.5 shows the values obtained alongwith the correlation coefficient and MPSD. An increase in Q from 0.02 to 0.04 L/min increased the β value due to the reduction in the film boundary layer surrounding the ACC particle at increased turbulence. Value of N_0 generally increased with increase in the value of Z, C_o and D, however, its value decreased with an increase in the value of Q. The predicted and experimental breakthrough curves showed good agreement between the experimental and predicted values for the relative concentration region up to 0.5.

5.3 CONTINUOUS ADSORPTION STUDY THROUGH BFA PACKED COLUMN

In order to study the removal of furfural through BFA packed column and for prediction of breakthrough curve, the continuous operations were performed. Here the effect of only three operational parameters (Z, C_o and Q) on shape of breakthrough curve, breakthrough time and on the adsorption capacity of ACC were investigated and presented here.

5.3.1 Effect of bed height (Z)

The breakthrough curves for furfural adsorption were investigated at four different Z (= 15, 30, 45 and 60 cm) at a constant Q = 0.02 L/min and C_o = 100 mg/L, and the results are shown in Fig. 5.22 by data points.

It was seen that initially, the furfural was rapidly adsorbed on BFA and the effluent (from the upper part of the bed) was almost free of furfural. As the furfural solution continued to flow, the BFA was progressively saturated with furfural, and therefore, the outlet concentration started to increase until the saturation point was reached. In practice, system operation is interrupted when the effluent concentration reaches a certain level, called breakthrough concentration, above which it is not profitable to continue the operation. In the present study, the experiments were performed until the saturation of the bed. When calculating the characteristic parameters of the system, a breakthrough concentration C_b (10% of C_o) was considered, and the time corresponding to this concentration was considered as breakthrough time ($t_{0.1}$).

It can be seen that the $t_{0.1}$ and the exhaustion time (t_e) were lowest for the lowest value of Z, and increased with an increase in the value of Z. This trend was due to the increase of the available surface area and binding sites for the furfural adsorption with an increase in the value of Z. The slope of breakthrough curve is also seen to decrease with an increase in the value of Z. This is due to the broadened mass transfer zone that makes breakthrough curves less steeper. The breakthrough curves for the lowest Z showed a very little "tail" towards saturation time because of the low quantity of the BFA inside the bed. As the value of Z increased, a steep S shape of breakthrough curve was observed. The broad tailing edge of the breakthrough curves at

higher Z is because of the rate limiting intra-particle diffusion mechanism [Cooney et al., 1999]. These results clearly reflect that the bed having greater value of Z was more difficult to completely exhaust as compared to bed having low value of Z [Zulfadhly et al., 2001; Netpradit et al., 2004].

5.3.2 Effect of feed concentration (C_o)

To investigate the effect C_o on breakthrough curves the values of Z and Q were kept constant at 60 cm and 0.02 L/min, respectively. The results are shown by data points in Fig. 5.23 and tabulated in Table 5.6. It is seen in figure that $t_{0.1}$ decreased with an increase in the C_o. At lower C_o, breakthrough curves were dispersed and breakthrough occurred slower. As the value of C_o increased, the slope of breakthrough increased. These results demonstrated that the change of concentration gradient affected the saturation rate and breakthrough time [Goel et al., 2005].

This occurs due to the fact that more adsorption sites are being covered with an increase in C_o. As the value of C_o increases, furfural loading rate increases, so does the driving force for mass transfer, which result in a decrease in the adsorption zone length [Han et al., 2002].

5.3.3 Effect of Flow rate (Q)

The breakthrough curves developed under the three different Q (= 0.02, 0.03 and 0.04 L/min) at constant Z (= 60 cm) and C_o (= 100 mg/L) were investigated. The experimental breakthrough times determined from Fig. 5.24 are shown in Table 5.6. As it can be observed from the figure that the value of $t_{0.1}$ decreased as the value of Q increased. In addition, decreasing Q resulted in the breakthrough curve broadening,

which in turn resulted in an increase in the difference between the breakthrough time and the saturation time. As expected, an increase in Q produces a diminution in breakthrough and exhaustion times, and as a consequence, the curves become steeper with a shorter mass transfer zone [Lodeiro et al., 2004].

5.3.4 Empty bed contact time and adsorbent usage rate

Choosing 10% breakthrough point as the treatment objective, the values of EBCT and U_r were determined using the data from the breakthrough curves obtained at various Z, Q and D and the results are given in Table 5.6. From these data, it can be seen that the value of U_r tends to increase with an increase in C_o. For C_o = 100 mg/L, packed bed operated at Q = 0.03 L/min and Z = 60 cm was found to have lowest U_r of 5.61 g/L with highest V_b of 14.67 L.

5.3.5 Application of Bed depth service time Model

Based on the data obtained at Q=0.02 L/min, plotting time for 50% breakthrough against bed height gives a linear relationship as seen in Fig. 5.25, in which the values predicted from the BDST model equation (3.16) are included for comparison. From the slopes of these lines, the adsorption capacity N_0 was calculated using equation. A 50% breakthrough curve between t and Z must result in a straight line passing through the origin, however, the straight line does not pass through the origin. The failure of $t_{0.5}$ versus Z curve passing through the origin indicates that the adsorption of furfural onto BFA occurs through complex mechanism, and more than one rate-limiting step is involved in the adsorption process [Sharma et al., 1995].

From the slopes of these lines, the adsorption capacity N_0 was calculated using Eq. (3.16). N_0 as calculated from the slope of 50% plot was 3473.54 mg/L. N_0 and k as calculated from the slope and the intercept of $t_{0.1}$ versus Z plot are found to be 3338.65 mg/L and 0.000562 L/mg min, respectively. N_0 values predicted by 10% breakthrough plot shows deviation of 3.88% as compared to the value predicted by 50% breakthrough plot.

Fig. 5.25 shows the experimental and theoretical breakthrough curves predicted by BDST model at various experimental conditions. It shows a very good fit to the data upto 50% adsorption of furfural. This suggests that the BDST model is valid for the relative concentration region up to 0.5. The values of N_0 and k as calculated from eq. (3.16) are tabulated in Table 5.6. It is seen that the value of k generally increase with an increase in Z and decrease in Q.

5.3.6 Application of Thomas Model

Thomas model was applied to the data at C/Co ratios higher than 0.08 and lower than 0.99 with respect to bed height and flow rate. Values of R^2 were found to be > 0.9063 (Table 5.7). k_{TH} and q_0 values are shown in Table 5.7. Fig. 5.26, 5.27, 5.28 shows the experimental and theoretical breakthrough curves obtained at varied bed heights, initial concentrations and flow rates for the Thomas model. It can be observed from the Table 5.7 that the values of q_0 shows any specific trend with the value of Z, Q and C_o. Table 5 shows that the values of ε are highest for the lowest value of Z and Co and for the highest value of Q, thus, this model gives poorer prediction of breakthrough point at these conditions.

5.3.7 Application of Yoon-Nelson Model

The values of k_{YN} and $t_{0.5}$ were determined from $\ln[C/(C_0 - C)]$ versus t at variable operating conditions. These values are listed in Table 5.8. Fig. 5.29, 5.30, 5.31 shows the experimental and theoretical breakthrough curves obtained at varied bed heights, initial concentrations and flow rates for the Yoon and Nelson model. The data in Table 5.8 indicate that the $t_{0.5}$ values as predicted from the Yoon and Nelson model matched very well to those predicted from experimental results. It can be observed from the Table 5.8 that the values of k_{YN} decreased with increased value of Z and increased with the increased value of C_o. However, it did not show any specific trend with respect to the value of Q. Table 5.8 shows that the values of ε are low thus, this model gives good prediction of breakthrough point at these conditions.

5.3.8 Application of Clark Model

Freundlich constant n = 5.123 [Sahu et al., 2008] has been used in the Clark model to calculate the model parameters for the adsorption of furfural on BFA column. Values of r and A in the Clark equation were determined from the slope and intercept of $\ln\left|(C_0/C)^{n-1} - 1\right|$ versus t plot according to Eq. (3.22). Fig. 5.32, 5.33, 5.34 shows the experimental and theoretical breakthrough curves obtained at varied bed heights, initial concentrations and flow rates for the Clark model. Table 5.9 shows the values obtained along with the correlation coefficient and MPSD. This model predicted the adsorption breakthrough well for C/Co > 1.5 with respect to all parameters. Below this level, this model could not be predicted the experimental data points. It appears that the

simulation of the whole breakthrough curve is impossible using Clark model. In our previous study [Sahu et al., 2008], it was found that the Langmuir model better represented the isotherm data as compared to Freundlich isotherm. Since, this model uses the Freundlich constant n as one of the input parameters which did not best represented the batch isotherm data, therefore, Clark model is not able to represent the breakthrough curve properly.

5.3.9 Application of Bohart Adams and Wolborska Model.

For determination of the fit of the Wolborska model, Eq. (3.27) was applied to the experimental data for varying operating parameters. A linear relationship between $\ln(C/C_0)$ and t was obtained for the relative concentration region up to 50% breakthrough. The kinetic coefficients of mass transfer as well as the bed capacity (N_0) were determined by the application of Bohart-Adams model. Fig. 5.35, 5.36, 5.37 show sthe experimental and theoretical breakthrough curves obtained atvvaried bed heights, initial concentrations and flow rates for the Bohart adams and Wolborska model. Table 5.10 shows the values obtained alongwith the correlation coefficient and MPSD. The predicted and experimental breakthrough curves showed good agreement between the experimental and predicted values for the relative concentration region up to 0.5.

Table 5.1: Comparison of fixed-bed performance of ACC for furfural adsorption.

Co (mg/L)	Q (L/min)	D (cm)	Z (cm)	EBCT (min)	T_b (min)	V_b (l)	N_b	U_r (g/l)
100	0.02	2.54	15	3.80	11.91	0.23	3.13	191.22
100	0.02	2.54	30	7.60	66.83	1.33	8.78	68.18
100	0.02	2.54	45	11.40	272.79	5.45	23.91	25.05
100	0.02	2.54	60	15.20	571.77	11.43	37.59	15.93
50	0.02	2.54	60	15.21	1279.47	25.58	84.14	7.12
100	0.02	2.54	60	15.21	571.78	11.43	37.60	15.94
200	0.02	2.54	60	15.21	425.79	8.51	28.00	21.41
100	0.02	2.54	60	15.20	571.77	11.43	37.59	15.93
100	0.03	2.54	60	10.13	253.75	7.6125	25.029	23.945
100	0.04	2.54	60	7.60	85.91	3.43	11.29	53.042
100	0.02	2	60	9.43	63.10	1.26	6.69	89.56
100	0.02	2.54	60	15.21	571.78	11.44	37.60	15.94
100	0.02	4	60	37.71	4168.62	83.37	110.53	5.42

Table 5.2: Parameters predicted by Thomas model for ACC packed column

Co (mg/L)	Q (L/min)	D (cm)	Z (cm)	k_{TH} x 10^{05} (l/mg min)	q_0 (mg/g)	$t_{b,cal}$ (min)	$t_{b,exp}$ (min)	ε	R^2	MPSD
100	0.02	2.54	15	5.44	1.09	-233.99	11.91	105.09	-0.8978	185.51
100	0.02	2.54	30	4.63	1.67	43.19	66.83	54.73	-0.9528	66.88
100	0.02	2.54	45	4.41	1.77	327.59	272.79	16.72	-0.9888	41.09
100	0.02	2.54	60	4.74	1.62	538.49	571.77	6.18	-0.9986	151.12
50	0.02	2.54	60	12.91	1.39	1373.88	1279.47	6.87	-0.9810	1602.93
100	0.02	2.54	60	4.75	1.62	538.50	571.78	6.18	-0.9986	422.73
200	0.02	2.54	60	2.63	2.84	458.38	425.79	7.10	-0.9979	420.99
100	0.02	2.54	60	4.75	1.62	538.49	571.77	6.18	-0.9986	2045.09
100	0.03	2.54	60	5.31	1.44	182.00	253.75	39.42	-0.9829	405.94
100	0.04	2.54	60	7.68	1.17	77.68	85.91	10.59	-0.9970	353.62
100	0.02	2	60	6.28	0.95	25.59	63.10	146.58	-0.9898	424.19
100	0.02	2.54	60	4.74	1.62	538.50	571.78	6.18	-0.9986	422.73
100	0.02	4	60	1.05	3.86	4025.64	4168.62	3.55	-0.9969	1429

Table 5.3: Parameters predicted by Yoon-Nelson model for ACC packed column

Co (mg/L)	Q (L/min)	D (cm)	Z (cm)	k_{YN} (min^{-1})	$t_{0.5,cal}$ (min)	$t_{0.5,exp}$ (min)	ε	R^2	MPSD
100	0.02	2.54	15	0.0054	169.70	120.57	28.95	0.8978	185.51
100	0.02	2.54	30	0.0046	517.62	555.90	7.39	0.9528	66.88
100	0.02	2.54	45	0.0044	824.86	870	5.47	0.9888	41.09
100	0.02	2.54	60	0.0047	1001.55	986.25	1.52	0.9986	151.12
50	0.02	2.54	60	0.00645	1714.31	1782.05	3.95	0.9810	339.60
100	0.02	2.54	60	0.00475	1001.56	986.25	1.52	0.9986	422.73
200	0.02	2.54	60	0.00525	876.76	911.38	3.94	0.9979	420.99
100	0.02	2.54	60	0.00475	1001.55	986.25	1.52	0.9986	431.64
100	0.03	2.54	60	0.00531	596.05	587.5	1.43	0.9829	405.94
100	0.04	2.54	60	0.00768	363.93	369.76	1.6	0.9970	353.62
100	0.02	2	60	0.0063	375.28	340.63	9.2	0.9898	424.19
100	0.02	2.54	60	0.0047	1001.56	986.25	1.52	0.9986	422.73
100	0.02	4	60	0.0011	6111.74	6237.14	2.05	0.9969	396.26

Table 5.4: Parameters predicted by Clark model for ACC packed column

Co (mg/L)	Q (L/min)	D (cm)	Z (cm)	r (min^{-1})	A	$t_{b,cal}$ (min)	$t_{b,exp}$ (min)	ε	R^2	MPSD
100	0.02	2.54	15	0.0074	23.42	-374.83	11.91	103.17	-0.7954	187.80
100	0.02	2.54	30	0.0066	234.23	-70	66.83	195.46	-0.9593	107.11
100	0.02	2.54	45	0.0065	1626.90	228.32	272.79	19.47	-0.9968	121.13
100	0.02	2.54	60	0.0066	5186.60	396.74	571.77	44.11	-0.9821	651.82
50	0.02	2.54	60	0.0097	152053713.4	1325.38	1279.47	3.46	-0.9956	279.13
100	0.02	2.54	60	0.0058	1041.16	178.24	571.78	220.79	-0.9912	1175.69
200	0.02	2.54	60	0.0077	7665.80	391.35	425.79	-8.80	-0.9901	703.97
100	0.02	2.54	60	0.0066	5186.60	396.74	571.77	44.11	-0.9821	874.71
100	0.03	2.54	60	0.0073	570.71	58.34	253.75	334.91	-0.9764	558.92
100	0.04	2.54	60	0.0116	527.06	30.15	85.91	184.95	-0.9893	446.93
100	0.02	2	60	0.0093	250.19	-42.58	63.10	248.19	-0.9741	505.98
100	0.02	2.54	60	0.0066	5186.61	396.75	571.78	44.11	-0.9821	856.66
100	0.02	4	60	0.0017	187878.60	3725.04	4168.62	11.90	-0.9898	764.37

Table 5.5: Parameters predicted by Bohart-Adams & Wolborska model for ACC packed column

Co (mg/L)	Q (L/min)	D (cm)	Z (cm)	N_0 (mg/L)	β (min^{-1})	$t_{b,cal}$ (min)	$t_{b,exp}$ (min)	ε	R^2	MPSD
100	0.02	2.54	15	4000.24	0.66	12.94	11.91	7.98	0.7464	94.89
100	0.02	2.54	30	8648.38	0.31	19.98	66.83	234.40	0.9028	133.12
100	0.02	2.54	45	9735.93	0.26	249.98	272.79	9.12	0.9917	174.45
100	0.02	2.54	60	7545.76	0.29	554.83	571.77	3.05	0.9884	326.27
50	0.02	2.54	60	6550.31	0.44	1310.40	1279.47	2.36	0.9925	283.90
100	0.02	2.54	60	7545.76	0.29	554.84	571.78	3.05	0.9884	724.10
200	0.02	2.54	60	14051.77	0.26	438.92	425.79	2.99	0.9775	749.89
100	0.02	2.54	60	7545.76	0.29	554.83	571.77	3.05	0.9884	739.35
100	0.03	2.54	60	7000.06	0.29	171.32	253.75	48.10	0.9167	716.52
100	0.04	2.54	60	6406.44	0.34	62.84	85.9127	36.71	0.9822	580.31
100	0.02	2	60	2983.01	0.17	41.37	63.10	52.52	0.9760	805.68
100	0.02	2.54	60	7545.76	0.29	554.84	571.78	3.05	0.9884	724.10
100	0.02	4	60	46311.49	0.34	3882.20	4168.62	7.37	0.9732	672.78

Table 5.6: Comparison of fixed-bed performance of BFA for furfural adsorption.

C_o (mg/L)	Q (L/min)	Z (cm)	EBCT (min)	t_b (min)	V_b (L)	N_b	U_r (g/L)
100	0.02	15	3.80	193.35	3.87	50.86	5.32
100	0.02	30	7.60	248.80	4.98	32.72	8.27
100	0.02	45	11.40	426.31	8.53	37.38	7.24
100	0.02	60	15.21	557.30	11.16	36.65	7.38
50	0.02	60	15.21	700.10	14.01	46.04	5.88
100	0.02	60	15.21	557.30	11.15	36.65	7.38
200	0.02	60	15.21	227.61	4.55	14.97	18.07
100	0.02	60	15.21	557.30	11.15	36.65	7.38
100	0.03	60	10.14	488.70	14.67	48.21	5.61
100	0.04	60	7.61	200.16	8.01	26.33	10.28

Table 5.7: Parameters predicted by Thomas model for BFA packed column

C_o (mg/L)	Q (L/min)	Z (cm)	$k_{TH} \times 10^5$ (L/mg min)	q_o (mg/g)	$t_{b,cal}$ (min)	$t_{b,exp}$ (min)	ε	R^2	MPSD
100	0.02	15	48.22	3.59	205.12	193.35	6.09	-0.9892	69.45
100	0.02	30	30.97	2.34	255.25	248.80	2.60	-0.9895	68.56
100	0.02	45	27.82	2.38	418.78	426.31	1.77	-0.9721	94.85
100	0.02	60	21.89	2.47	587.77	557.30	5.47	-0.9370	152.35
50	0.02	60	14.05	1.72	646.04	700.10	7.72	-0.9063	684.01
100	0.02	60	21.89	2.47	587.77	557.30	5.47	-0.9370	427.13
200	0.02	60	11.38	2.34	229.79	227.61	0.96	-0.9801	359.89
100	0.02	60	21.89	2.46	587.77	557.30	5.47	-0.9370	436.13
100	0.03	60	23.27	3.28	514.62	488.70	5.30	-0.9871	356.57
100	0.04	60	20.33	2.19	197.06	200.17	1.54	-0.9856	680.92

Table 5.8: Parameters predicted by Yoon-Nelson model for BFA packed column

Co (mg/L)	Q (L/min)	D (cm)	Z (cm)	k_{YN} (min^{-1})	$t_{0.5}$ (cal) (min)	$t_{0.5}$ (exp) (min)	ε	R^2	MPSD
100	0.02	2.54	15	0.048	250.69	260.97	3.94	0.9892	185.51
100	0.02	2.54	30	0.031	326.21	309.74	5.31	0.9895	66.88
100	0.02	2.54	45	0.028	497.77	479.41	3.83	0.9721	41.09
100	0.02	2.54	60	0.022	688.17	644.61	6.76	0.9370	151.12
50	0.02	2.54	60	0.006	958.86	854.98	12.2	0.9063	339.60
100	0.02	2.54	60	0.022	688.17	644.61	6.76	0.9370	422.73
200	0.02	2.54	60	0.023	326.33	307.44	6.15	0.9801	420.99
100	0.02	2.54	60	0.022	688.17	644.61	6.76	0.9370	431.64
100	0.03	2.54	60	0.024	609.06	590.08	3.22	0.9871	405.94
100	0.04	2.54	60	0.021	305.16	288.77	5.68	0.9856	353.62

Table 5.9: Parameters predicted by the Clark model for BFA packed column

Co (mg/L)	Q (L/min)	D (cm)	Z (cm)	r (min^{-1})	A	$t_{b,cal}$ (min)	$t_{b,exp}$ (min)	ε	R^2	MPSD
100	0.02	2.54	15	0.0999	1.63×10^{13}	209.45	193.35	8.33	-0.9690	187.80
100	0.02	2.54	30	0.0622	6.81×10^{10}	248.24	248.8	0.23	-0.9189	107.11
100	0.02	2.54	45	0.0560	1.18×10^{14}	409.03	426.31	4.06	-0.8958	121.13
100	0.02	2.54	60	0.0513	3.44×10^{17}	601.69	557.3	7.97	-0.8126	651.82
50	0.02	2.54	60	0.014	2.69×10^{7}	621.06	700.10	11.29	-0.7815	279.13
100	0.02	2.54	60	0.052	3.44×10^{17}	601.69	557.30	-7.96	-0.8126	1175.69
200	0.02	2.54	60	0.045	2.29×10^{8}	220.13	227.61	3.28	-0.8928	703.97
100	0.02	2.54	60	0.052	3.44×10^{17}	601.69	557.3	7.97	-0.8126	874.71
100	0.03	2.54	60	0.056	5.85×10^{16}	523.92	488.7	7.21	-0.9338	558.92
100	0.04	2.54	60	0.042	2.48×10^{7}	180.20	200.16	9.97	-0.9207	446.93

Table 5.10: Parameters predicted by Adam-Bohart & Wolborska model for BFA packed column

C_o (mg/L)	Q (L/min)	Z (cm)	$k_{AB \times 10^5}$ (L/mg min)	N_0 (mg/L)	$t_{b,cal}$ (min)	$t_{b,exp}$ (min)	ε	R^2	MPSD
100	0.02	15	26.97	7775.59	210.12	193.35	8.68	0.9501	60.75
100	0.02	30	24.65	4704.22	264.12	248.80	6.16	0.9419	71.09
100	0.02	45	37.70	4369.32	437.08	426.31	2.50	0.9813	80.12
100	0.02	60	37.94	4341.25	599.25	557.30	7.50	0.9133	92.92
50	0.02	60	24.38	3069.48	744.33	700.10	6.32	0.8883	436.43
100	0.02	60	37.94	4341.25	599.25	557.30	7.53	0.9133	429.62
200	0.02	60	13.17	4444.12	250.37	227.61	10.00	0.9647	326.99
100	0.02	60	37.94	4341.25	599.25	557.30	7.53	0.9133	438.67
100	0.03	60	19.42	6408.52	530.97	488.70	8.65	0.9748	377.64
100	0.04	60	17.94	4455.56	210.29	200.16	5.06	0.9531	570.54

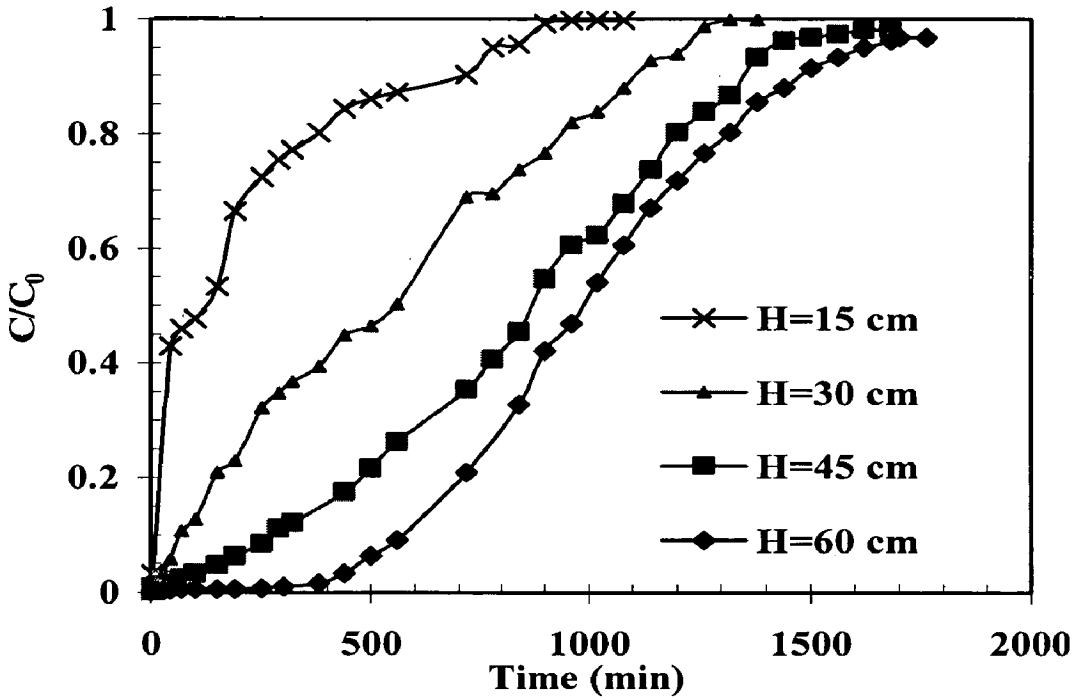

Fig. 5.1: Experimental breakthrough curves for furfural sorption on ACC packed column at varied bed lengths

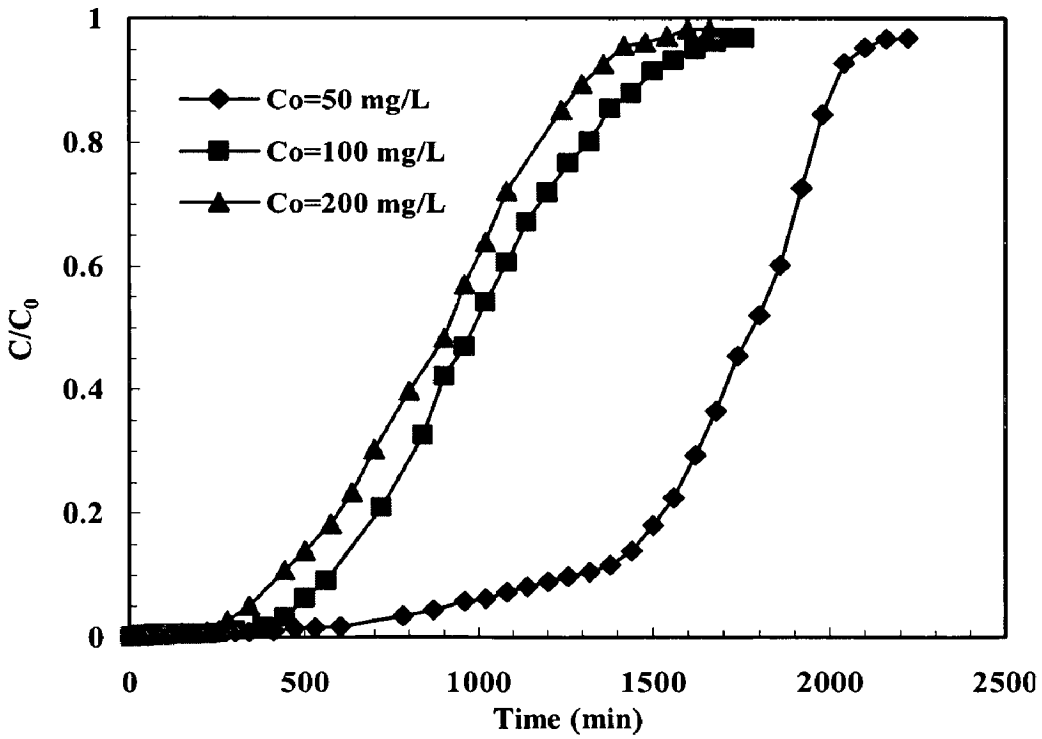

Fig. 5.2: Experimental breakthrough curves for furfural sorption on ACC packed column at varied initial concentrations.

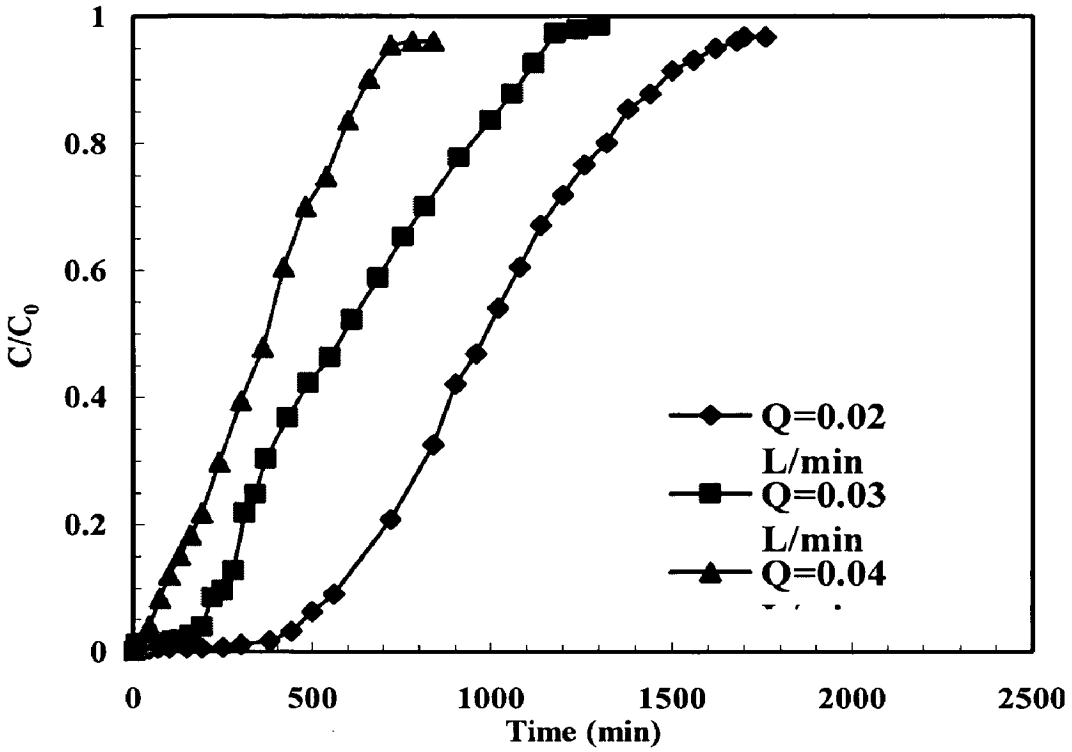

Fig. 5.3: Experimental breakthrough curves for furfural sorption on ACC packed column at varied flow rates.

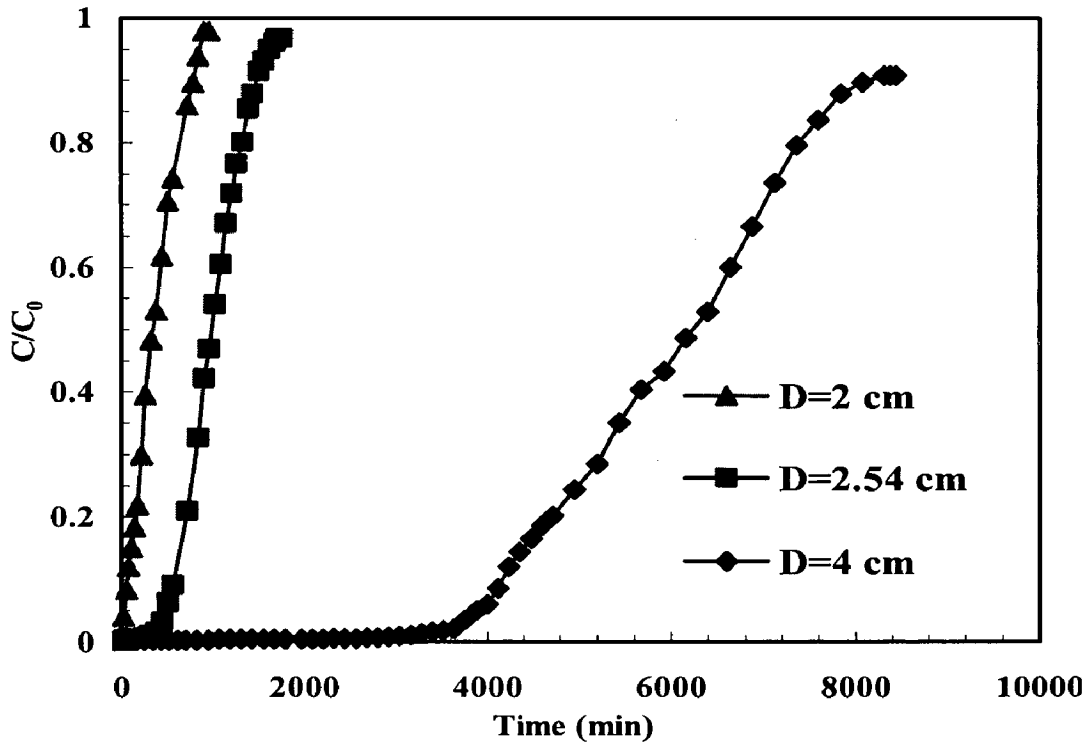

Fig. 5.4: Experimental breakthrough curves for furfural sorption on ACC packed column at varied column diameters

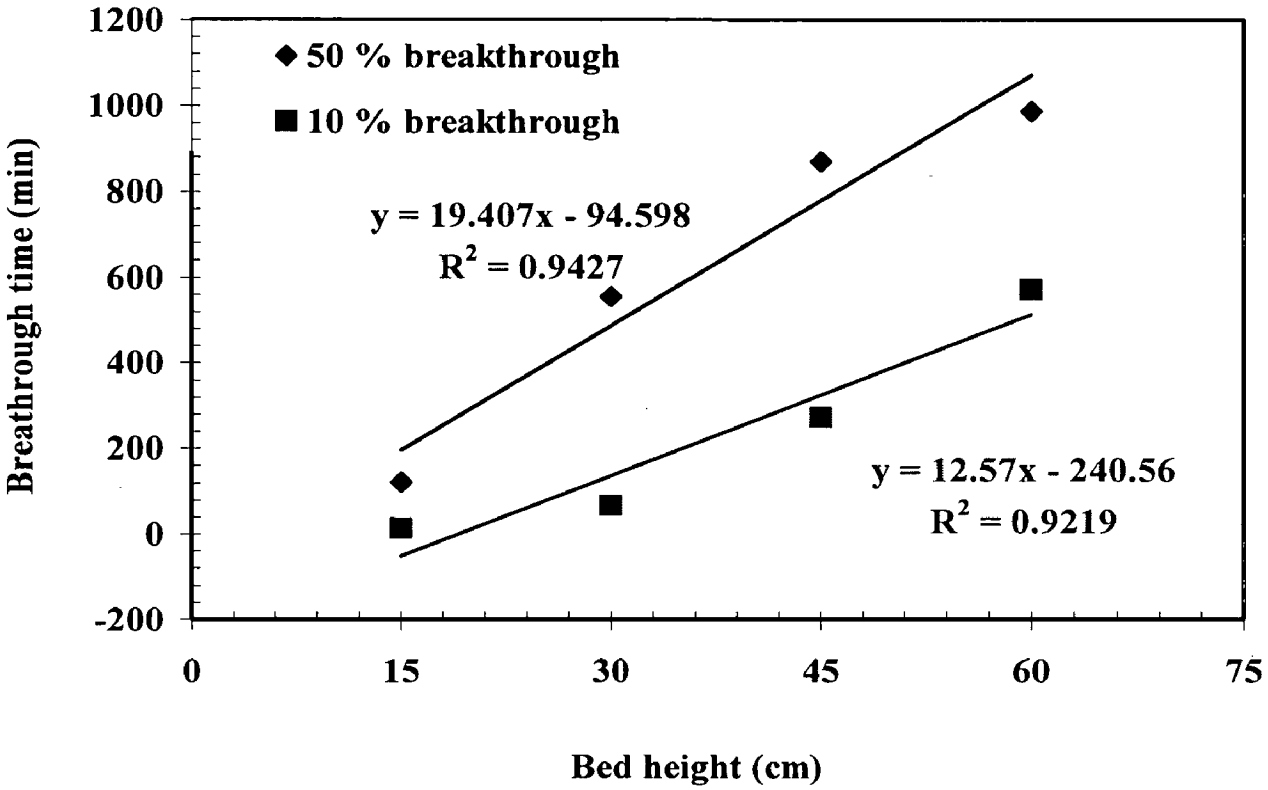

Fig. 5.5: Time for breakthrough compared to bed length for furfural adsorption on a ACC packed column according to the BDST model.

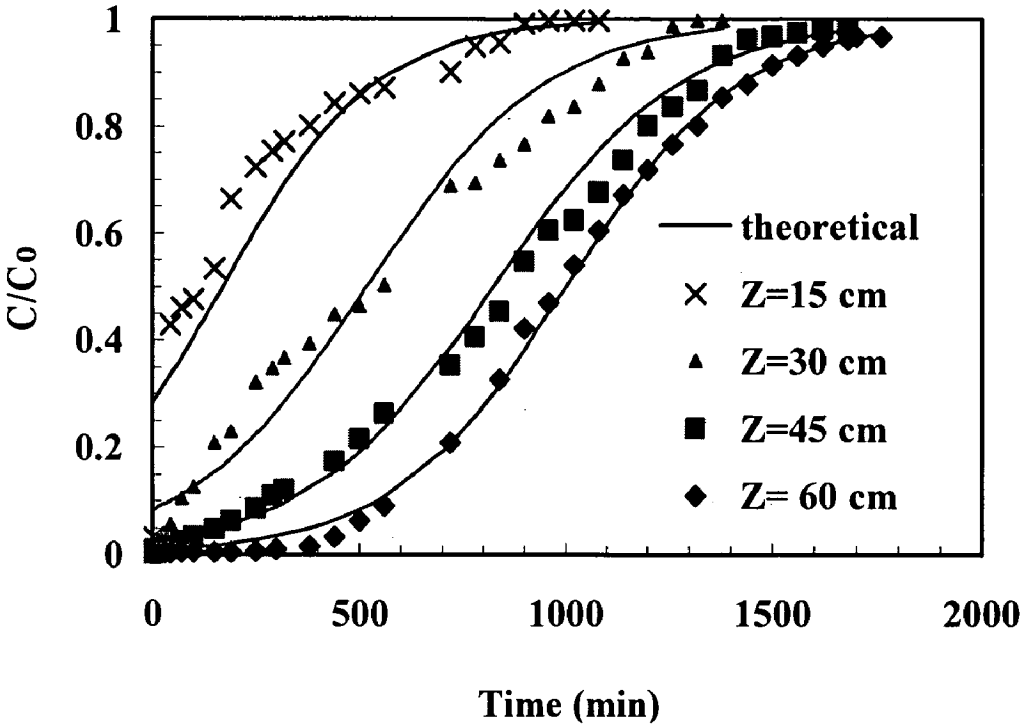

Fig. 5.6: Comparison of experimental and theoretical breakthrough curves for furfural sorption on ACC packed column using the Thomas model at varied bed lengths

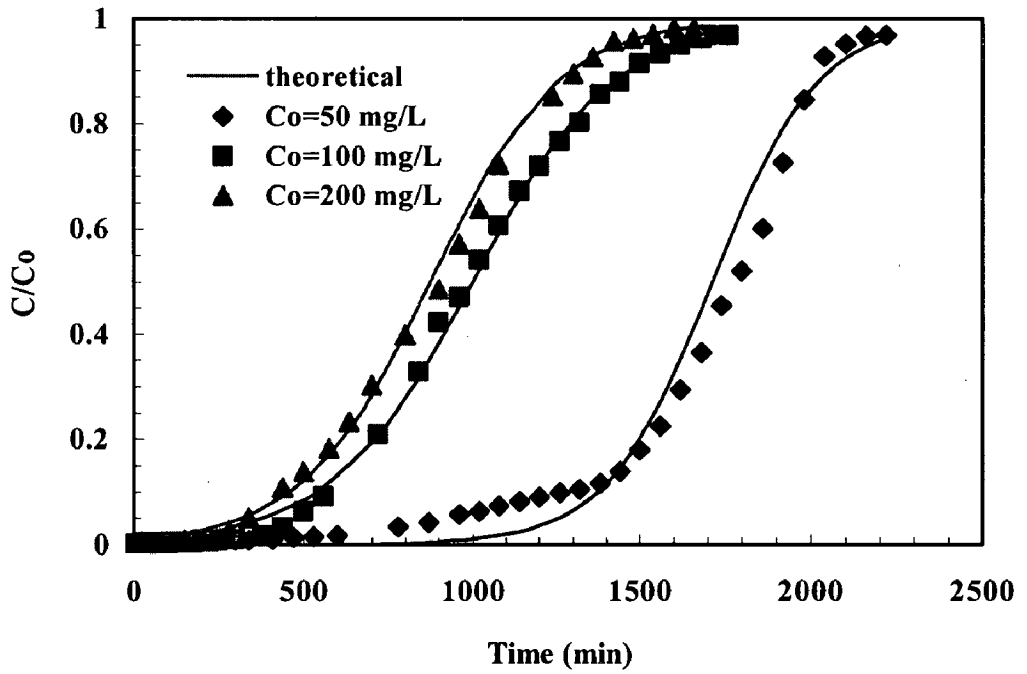

Fig. 5.7: Comparison of experimental and theoretical breakthrough curves for furfural sorption on ACC packed column using the Thomas model at varied initial concentrations

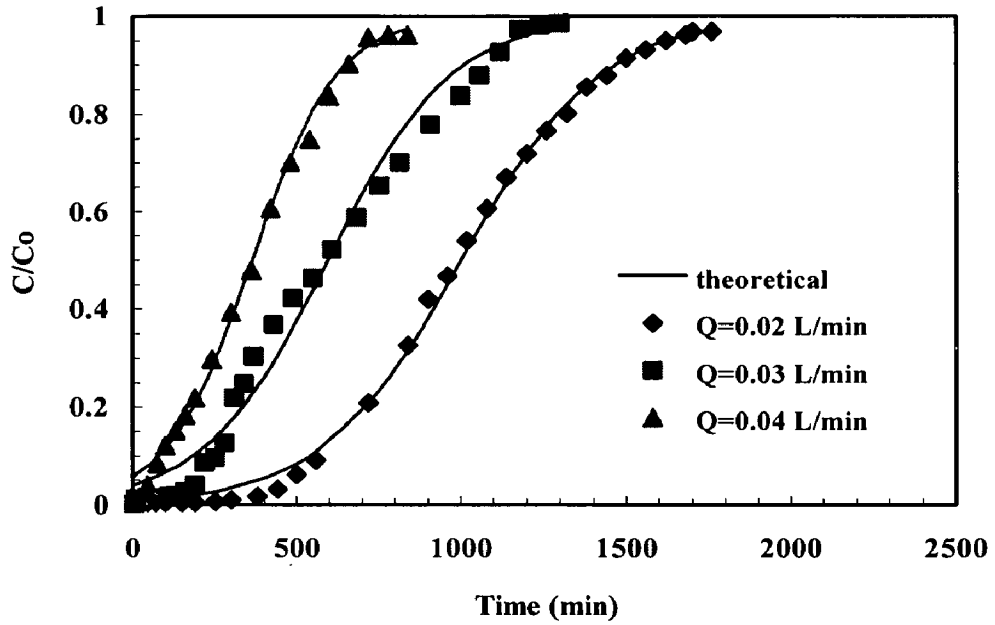

Fig. 5.8: Comparison of experimental and theoretical breakthrough curves for furfural sorption on ACC packed column using the Thomas model at varied flow rates

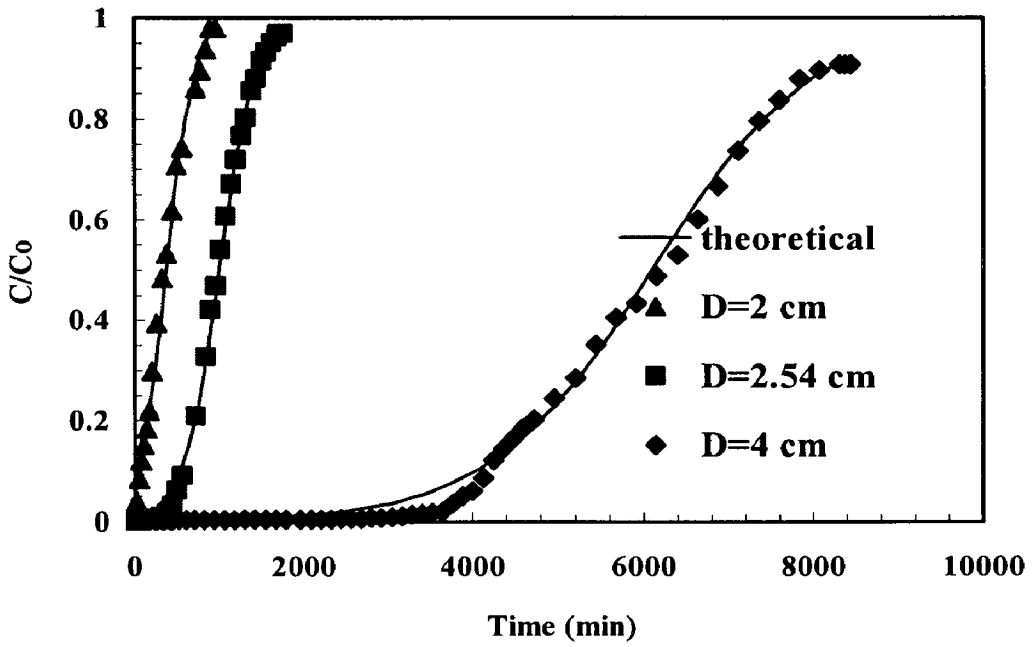

Fig. 5.9: Comparison of experimental and theoretical breakthrough curves for furfural sorption on ACC packed column using the Thomas model at varied column diameters

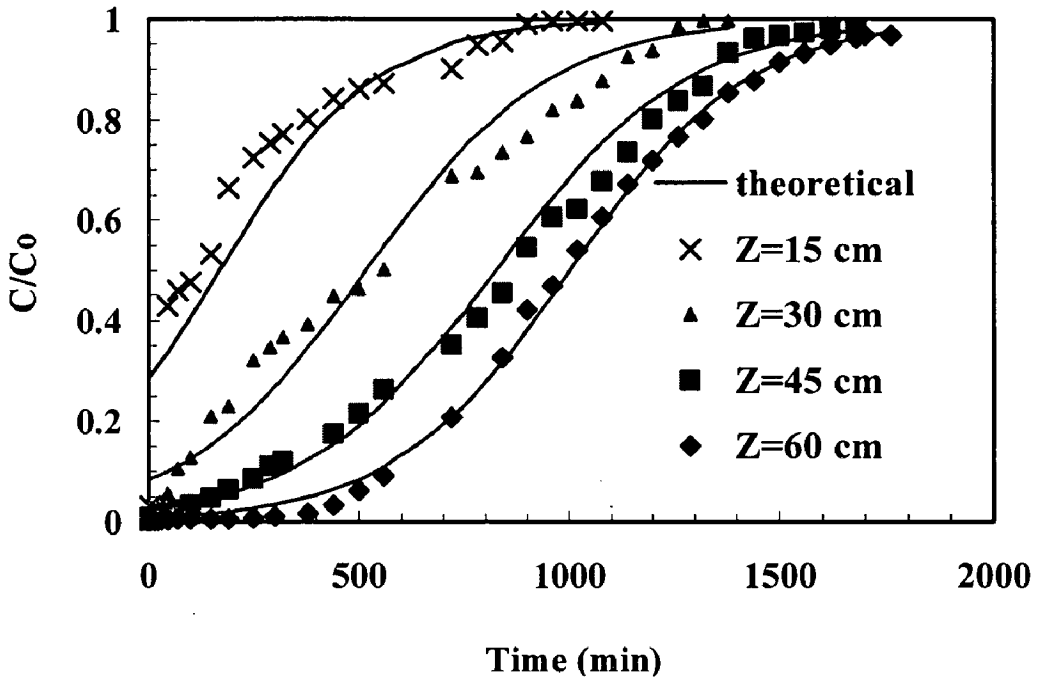

Fig. 5.10: Comparison of experimental and theoretical breakthrough curves for furfural sorption on ACC packed column using the Yoon-Nelson model at varied bed lengths

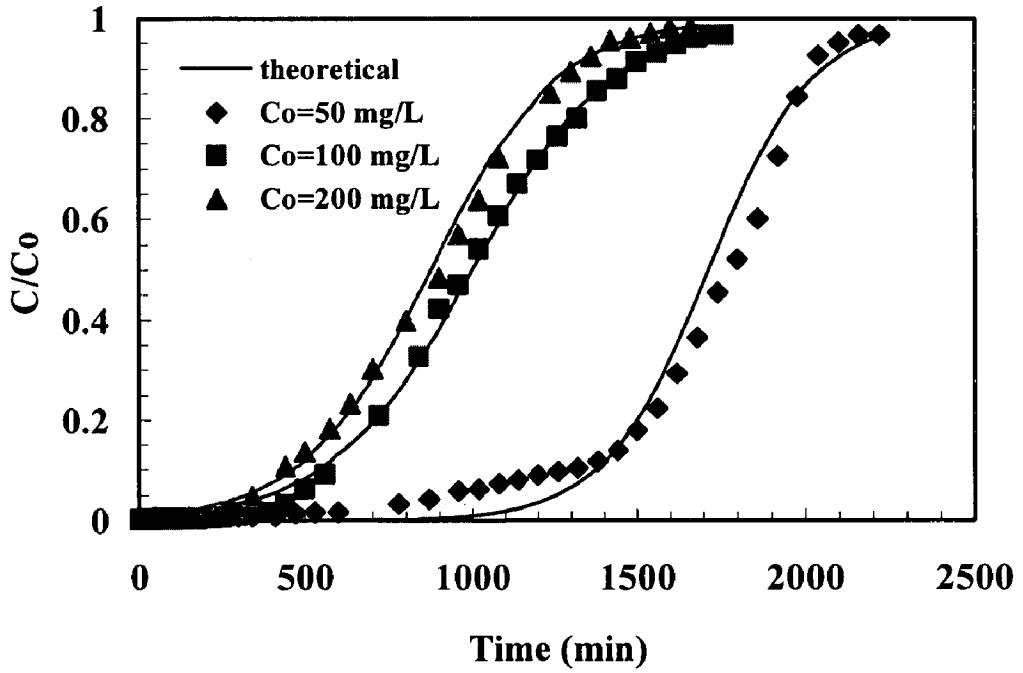

Fig. 5.11: Comparison of experimental and theoretical breakthrough curves for furfural sorption on ACC packed column using the Yoon-Nelson model at varied initial concentrations.

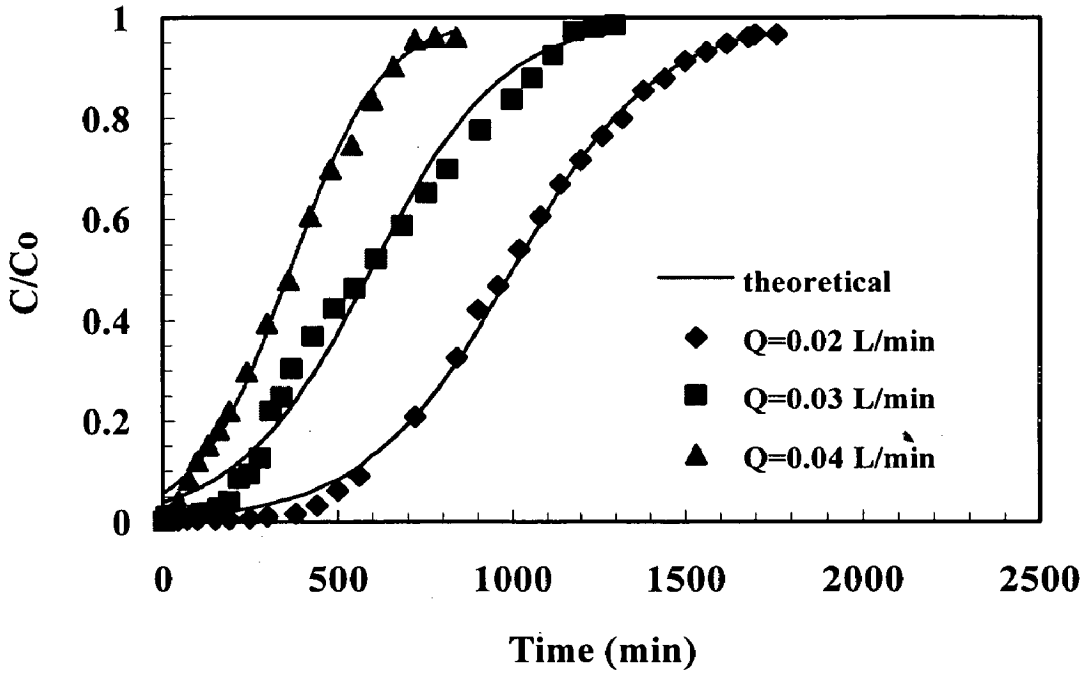

Fig. 5.12: Comparison of experimental and theoretical breakthrough curves for furfural sorption on ACC packed column using the Yoon-Nelson model at varied flow rates

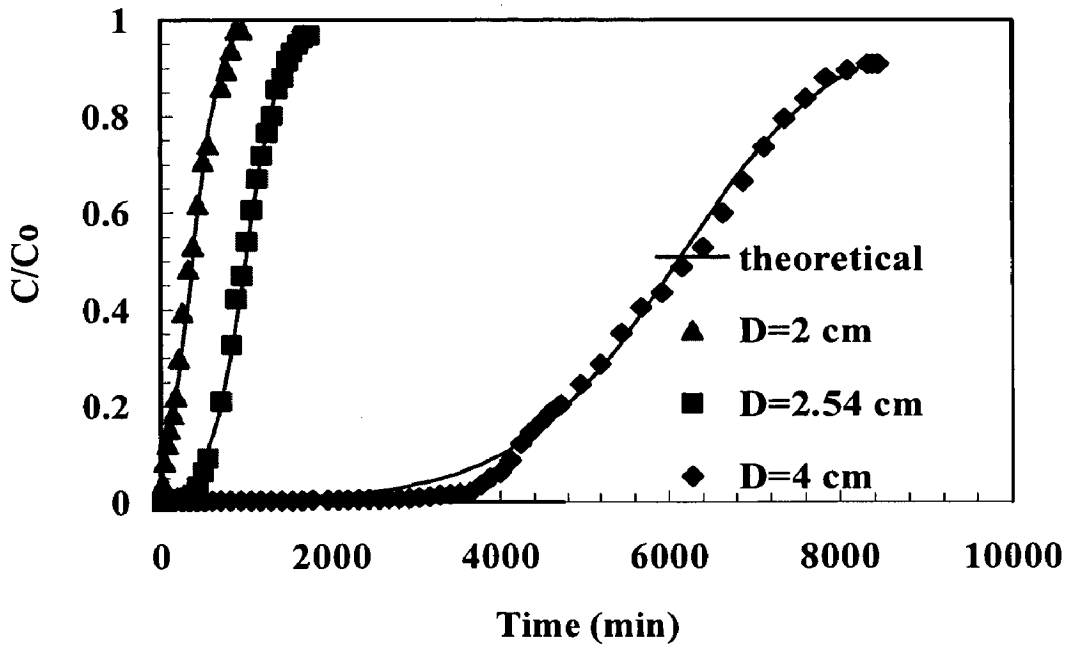

Fig. 5.13: Comparison of experimental and theoretical breakthrough curves for furfural sorption on ACC packed column using the Yoon-Nelson model at varied column diameters

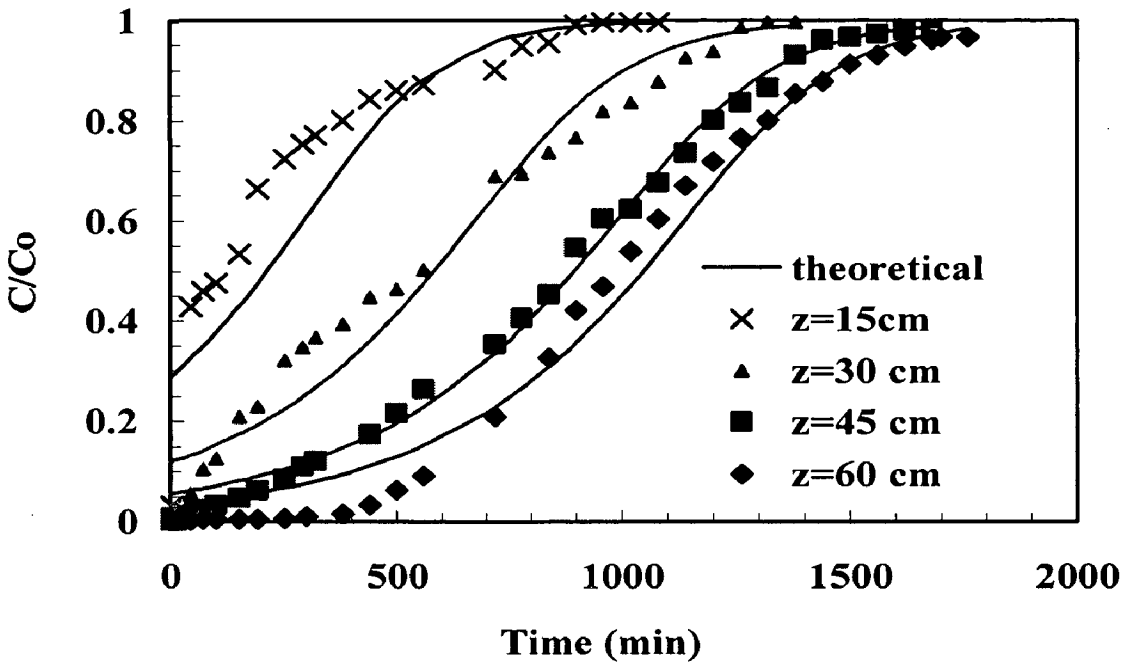

Fig. 5.14: Comparison of experimental and theoretical breakthrough curves for furfural sorption on ACC packed column using the Clark model. at varied bed lengths.

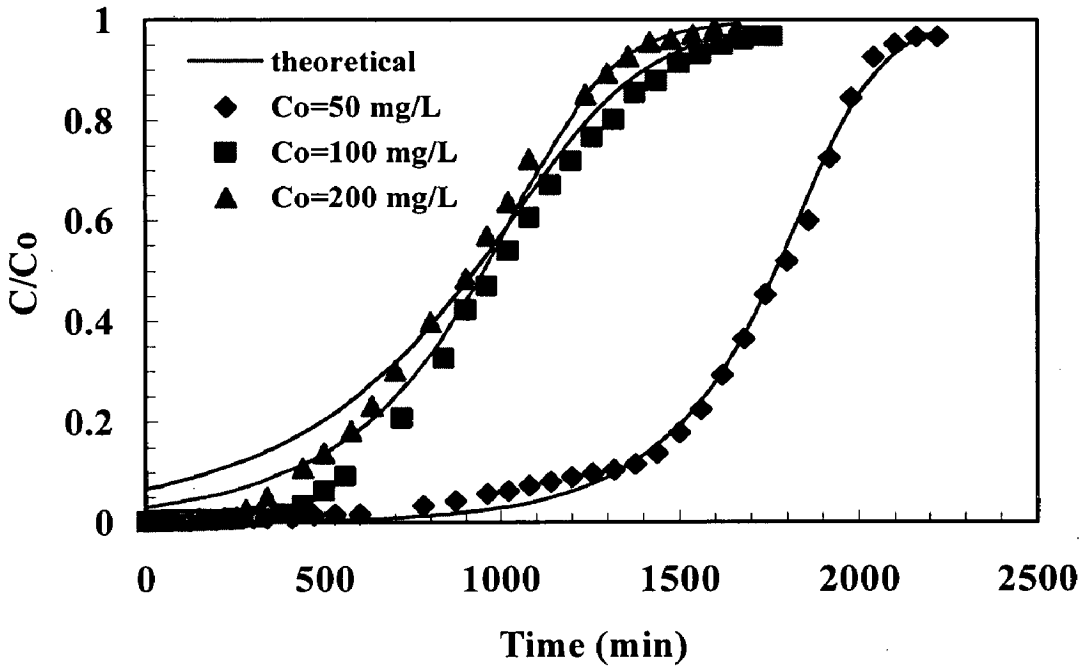

Fig. 5.15: Comparison of experimental and theoretical breakthrough curves for furfural sorption on ACC packed column using the Clark model at varied initial concentrations

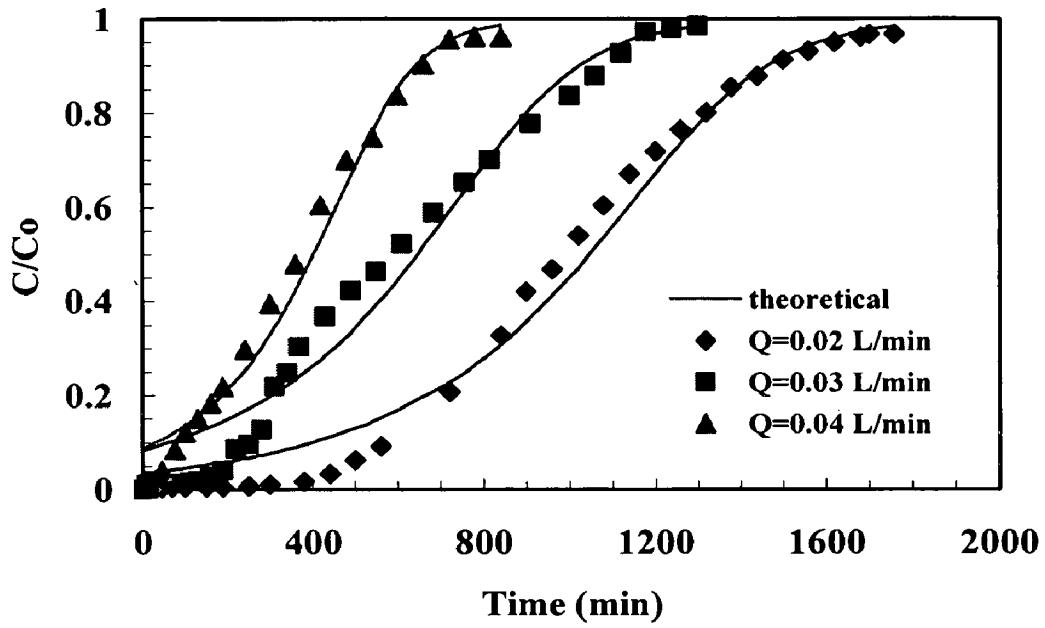

Fig. 5.16: Comparison of experimental and theoretical breakthrough curves for furfural sorption on ACC packed column using the Clark model at varied flow rates

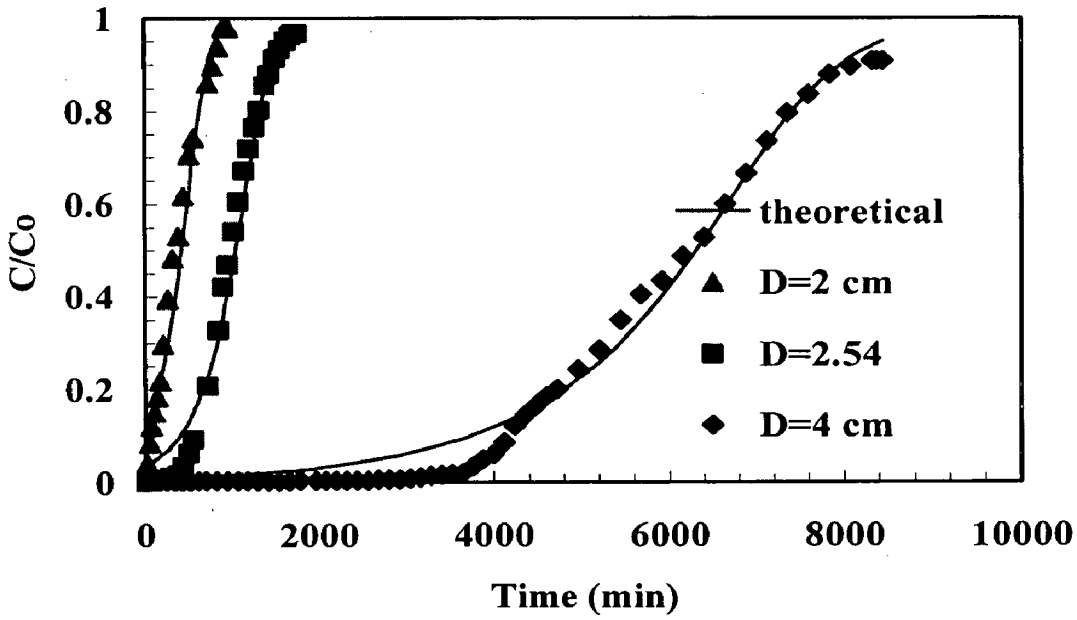

Fig. 5.17: Comparison of experimental and theoretical breakthrough curves for furfural sorption on ACC packed column using the Clark model at varied column diameters

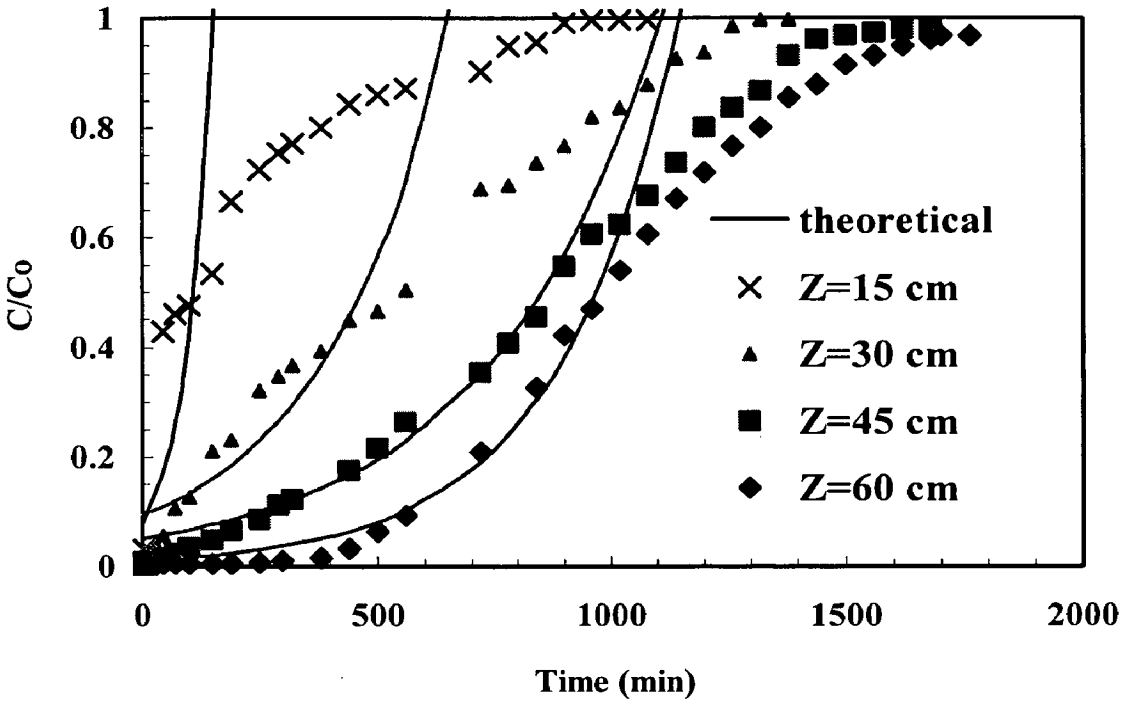

Fig. 5.18: Comparison of experimental and theoretical breakthrough curves for furfural sorption on ACC packed column using the Bohart-adams & Wolborska model at varied bed lengths

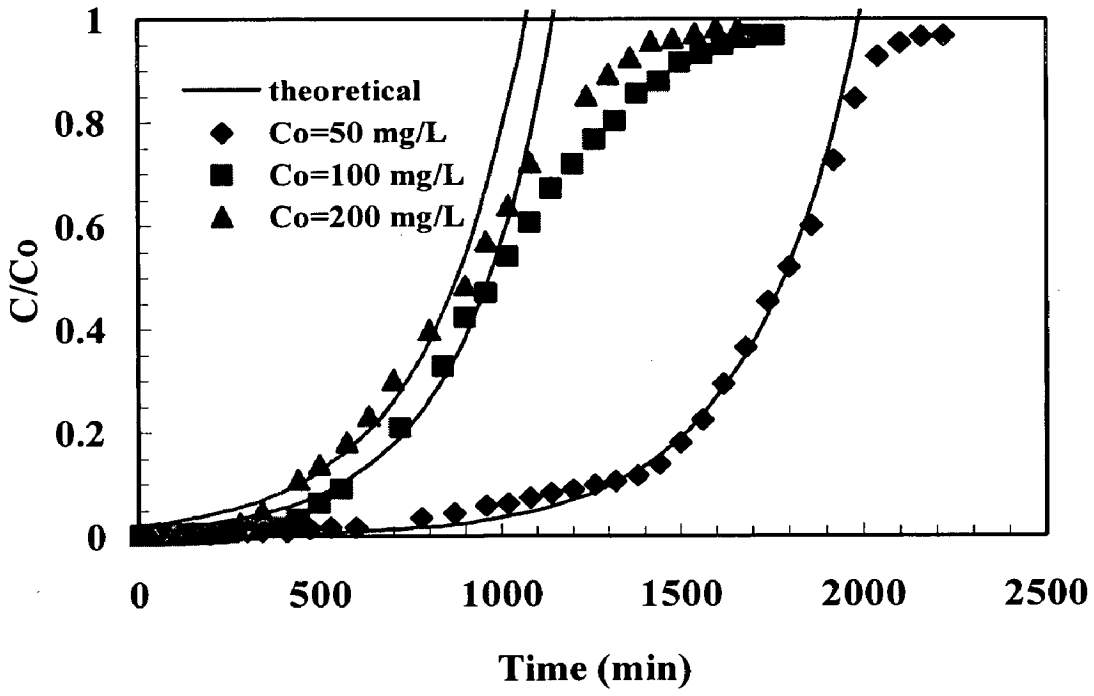

Fig. 5.19: Comparison of experimental and theoretical breakthrough curves for furfural sorption on ACC packed column using the Bohart-adams & Wolborska model at varied initial concentrations.

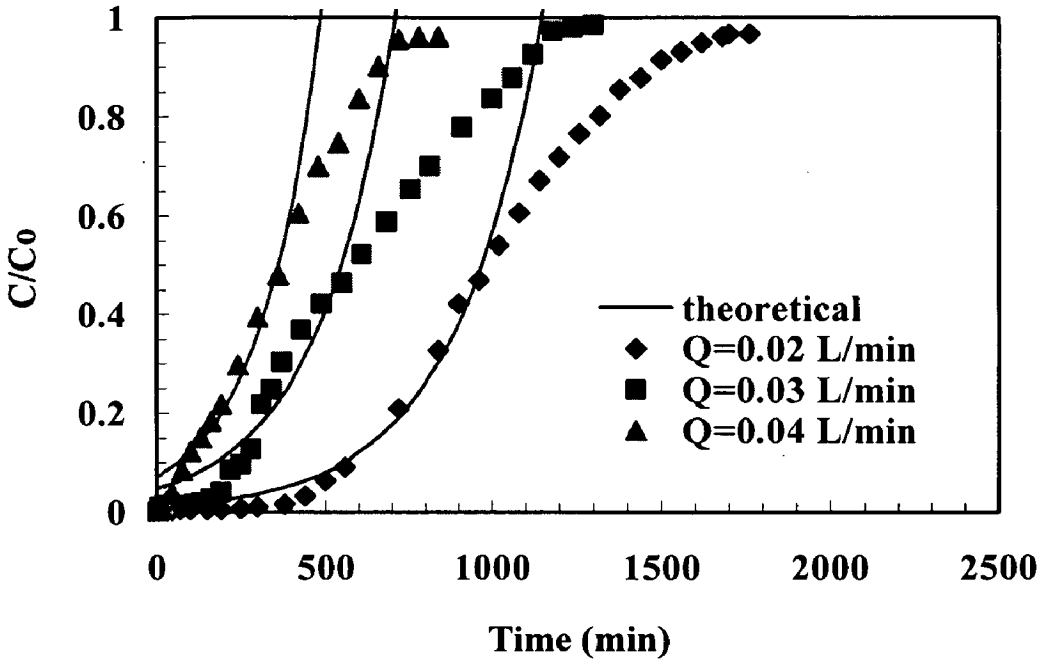

Fig. 5.20: Comparison of experimental and theoretical breakthrough curves for furfural sorption on ACC packed column using the Bohart-adams & Wolborska model at varied flow rates

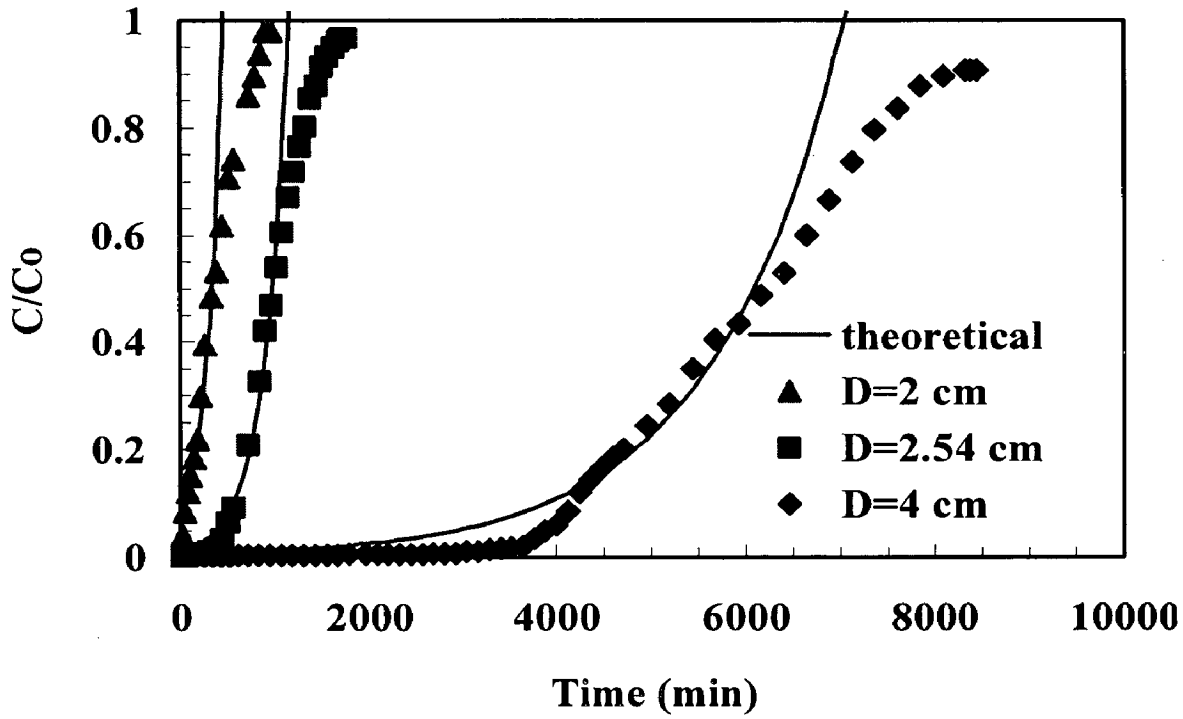

Fig. 5.21: Comparison of experimental and theoretical breakthrough curves for furfural sorption on ACC packed column using the Bohart-adams & Wolborska model at varied column diameters.

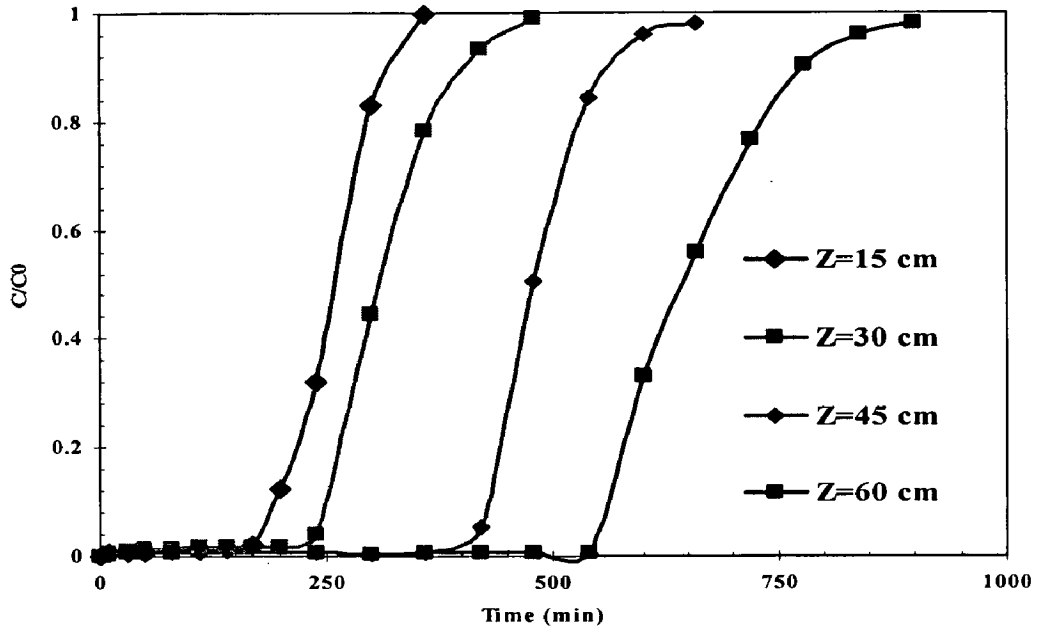

Fig. 5.22: Experimental breakthrough curves for furfural sorption on BFA packed column at varied bed lengths

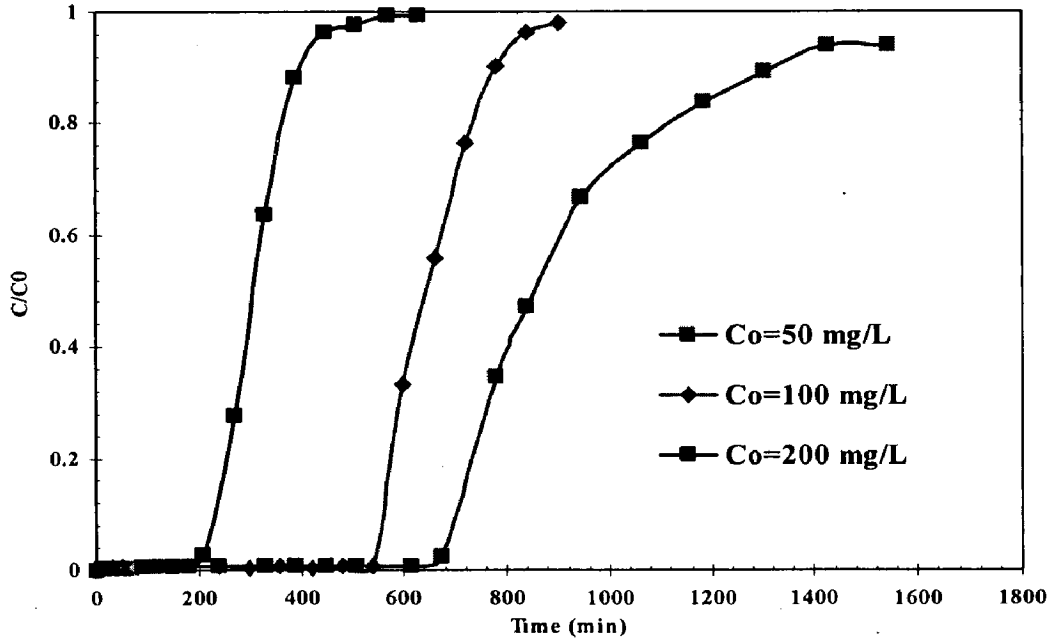

Fig. 5.23: Experimental breakthrough curves for furfural sorption on BFA packed column at varied initial concentrations.

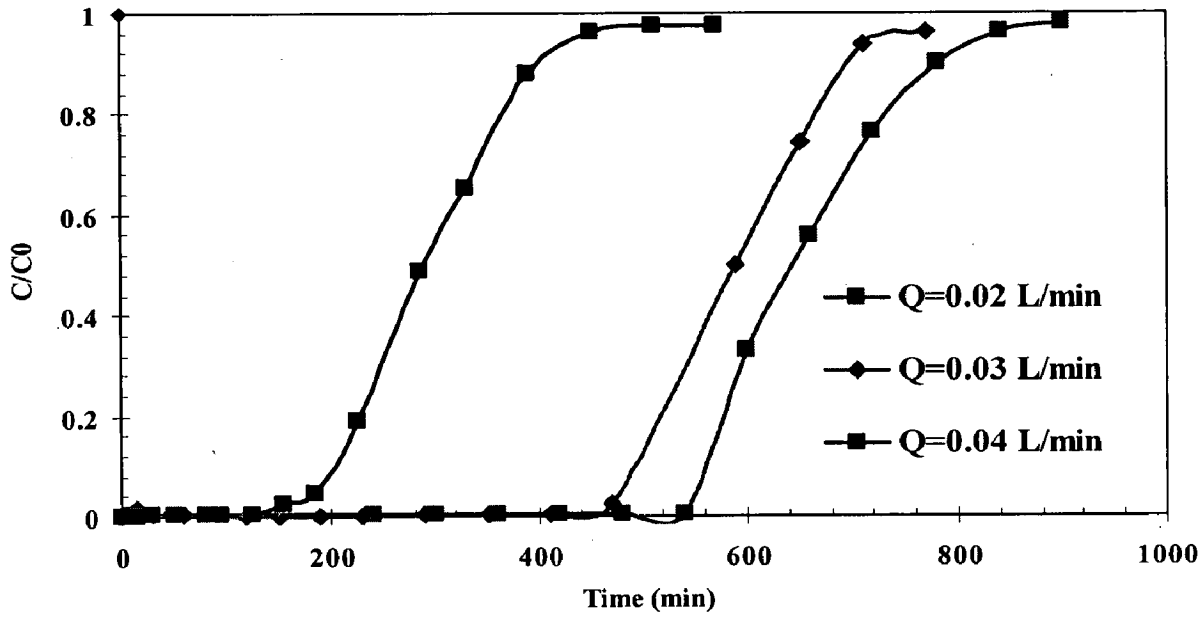

Fig. 5.24: Experimental breakthrough curves for furfural sorption on BFA packed column at varied flow rates.

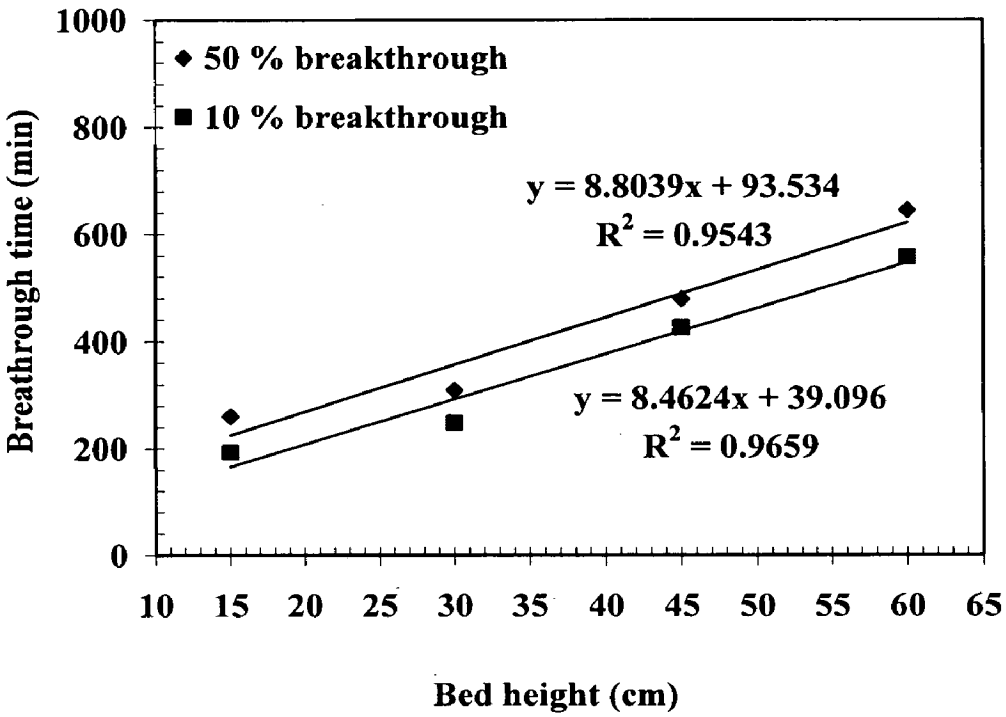

Fig. 5.25: Time for breakthrough compared to bed length for furfural adsorption on a BFA packed column according to the BDST model.

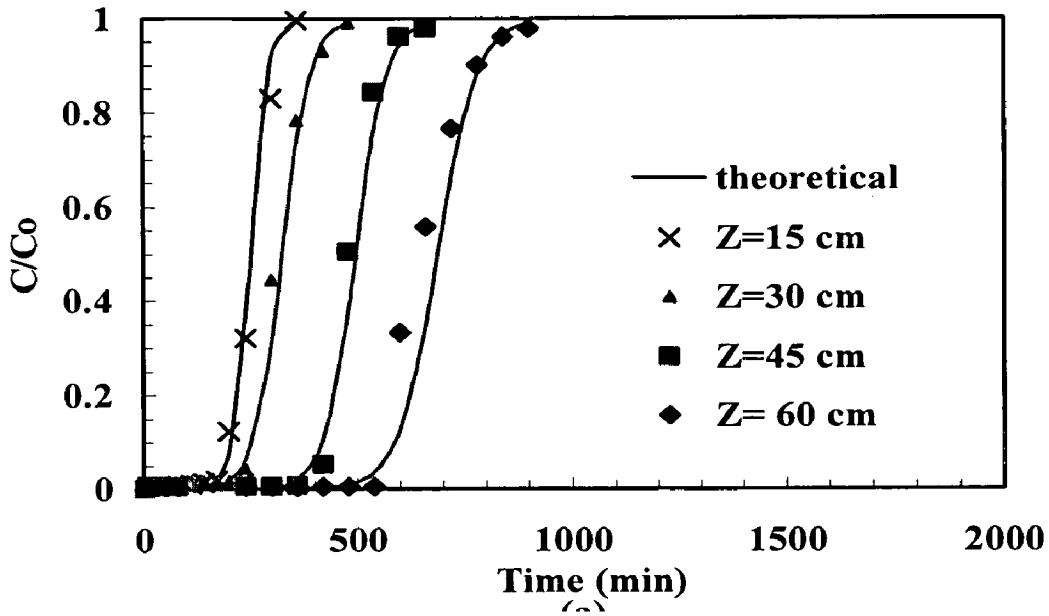

Fig. 5.26: Comparison of experimental and theoretical breakthrough curves for furfural sorption on BFA packed column using the Thomas model at varied bed lengths

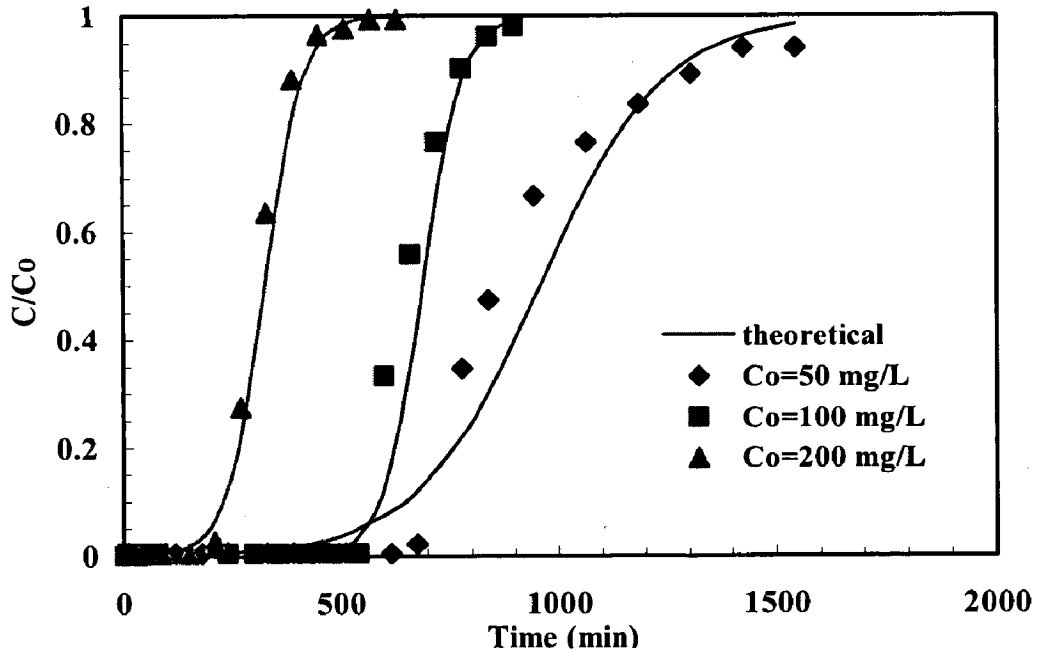

Fig. 5.27: Comparison of experimental and theoretical breakthrough curves for furfural sorption on BFA packed column using the Thomas model at varied initial concentrations

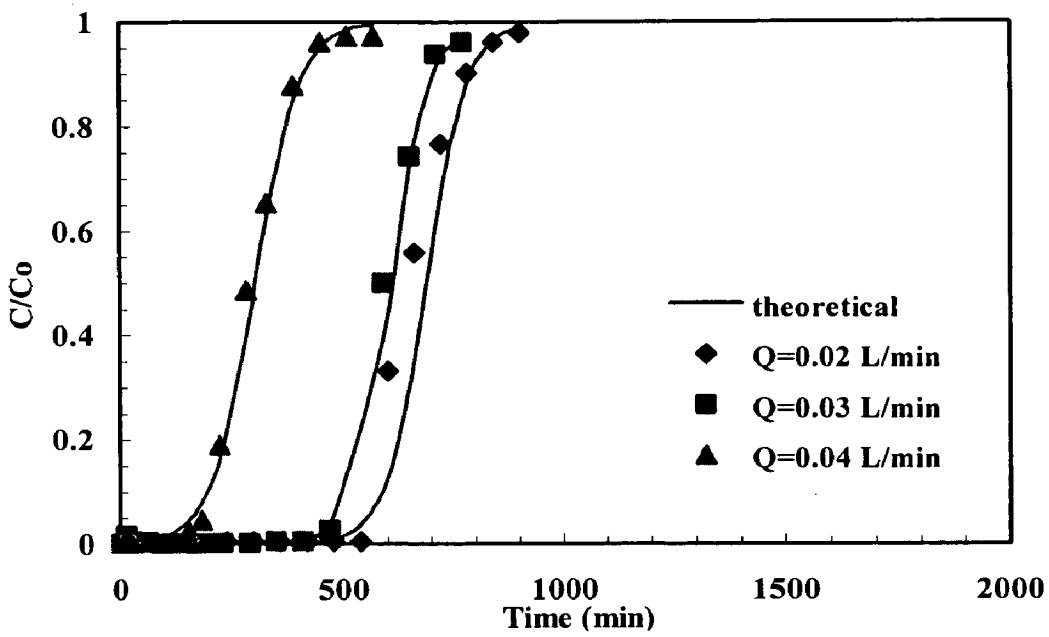

Fig. 5.28: Comparison of experimental and theoretical breakthrough curves for furfural sorption on BFA packed column using the Thomas model at varied flow rates.

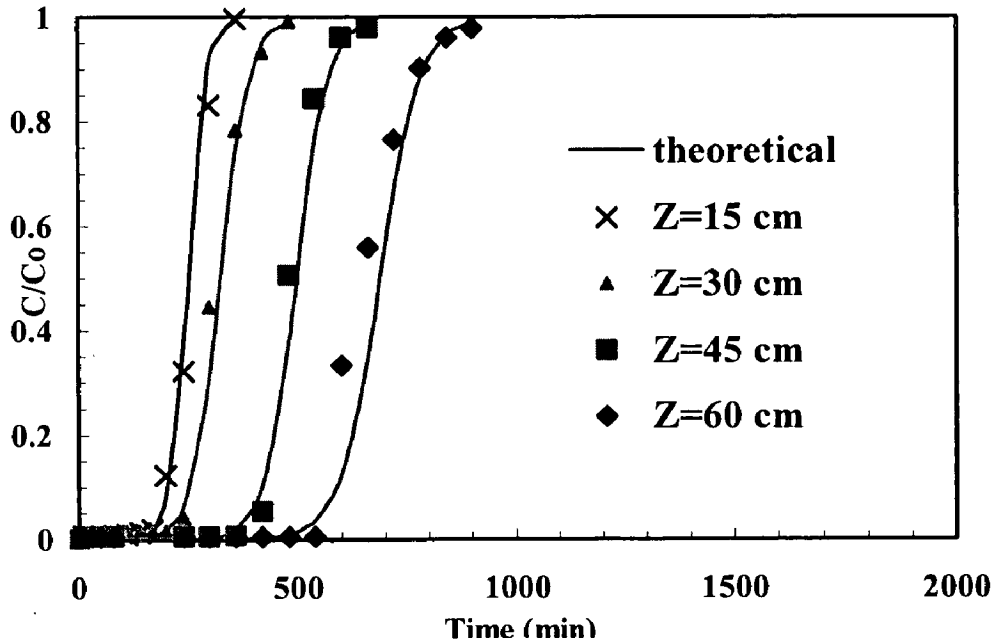

Fig. 5.29: Comparison of experimental and theoretical breakthrough curves for furfural sorption on BFA packed column using the Yoon-Nelson model at varied bed lengths

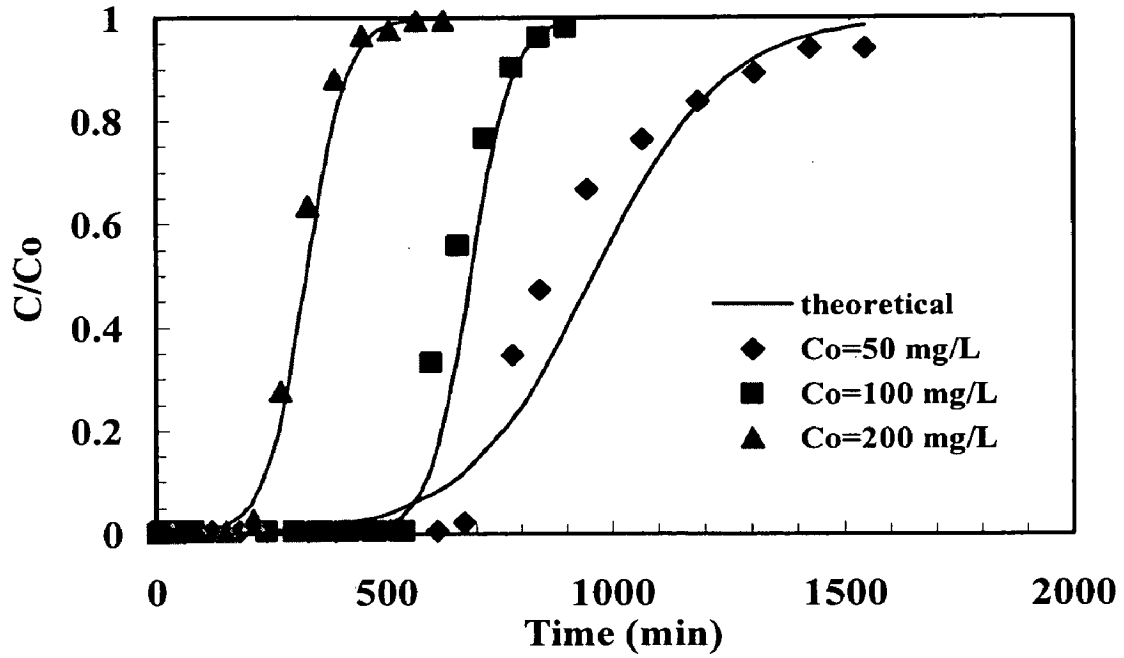

Fig. 5.30: Comparison of experimental and theoretical breakthrough curves for furfural sorption on BFA packed column using the Yoon-Nelson model at varied initial concentrations.

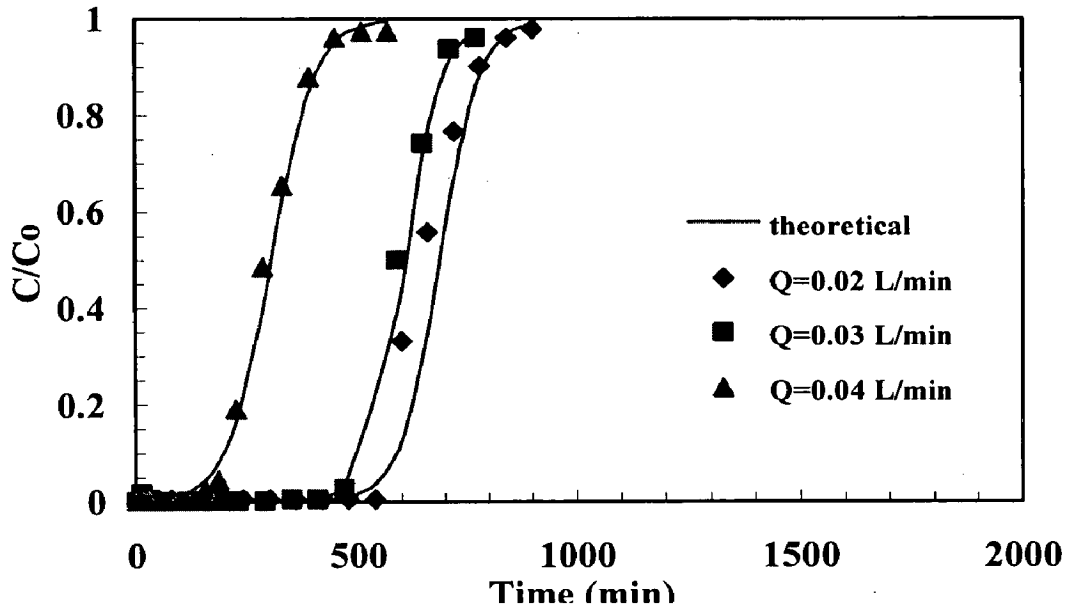

Fig. 5.31: Comparison of experimental and theoretical breakthrough curves for furfural sorption on BFA packed column using the Yoon-Nelson model at varied flow rates.

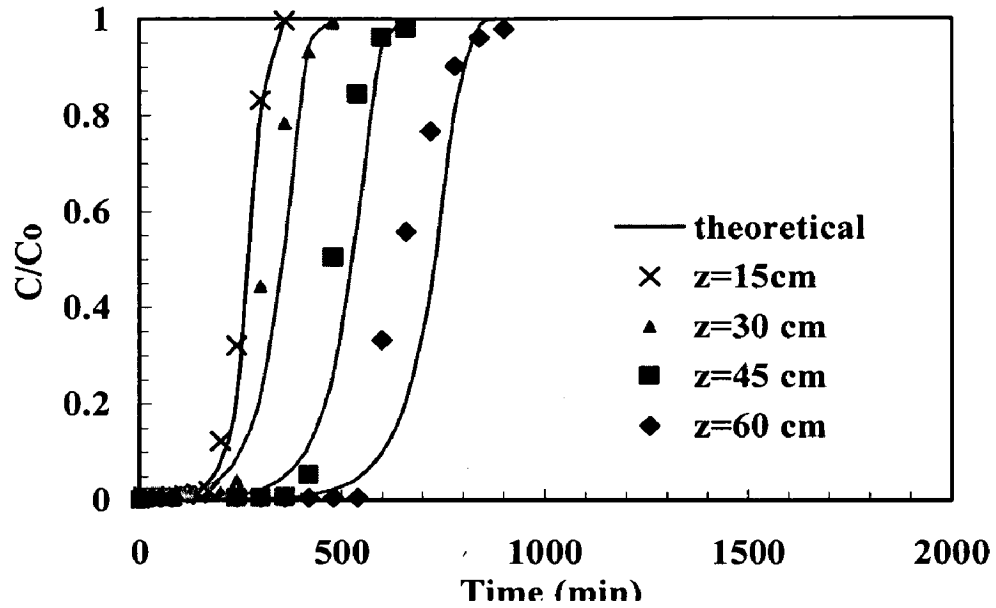

Fig. 5.32: Comparison of experimental and theoretical breakthrough curves for furfural sorption on BFA packed column using the Clark model at varied bed lengths.

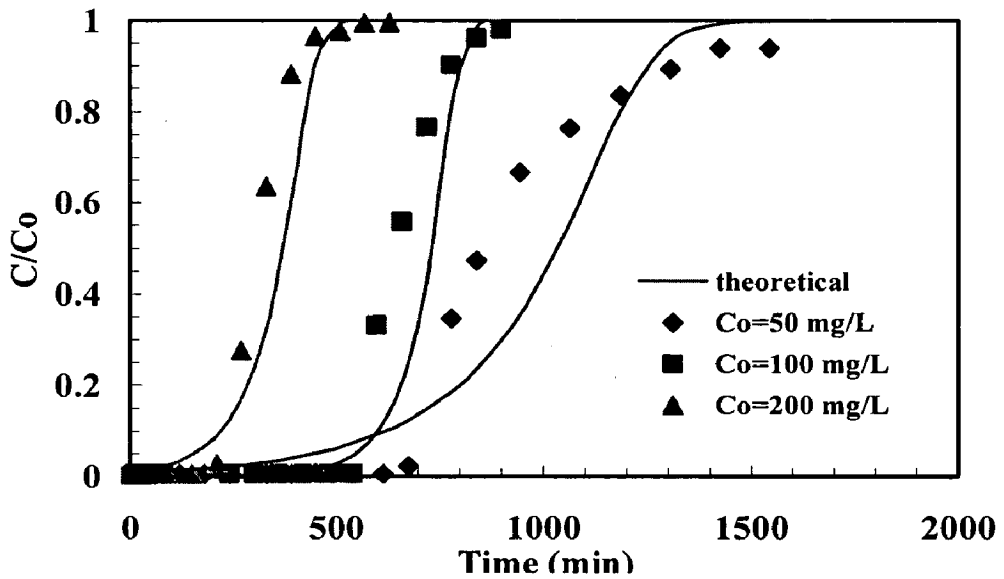

Fig. 5.33: Comparison of experimental and theoretical breakthrough curves for furfural sorption on BFA packed column using the Clark model at varied initial concentrations.

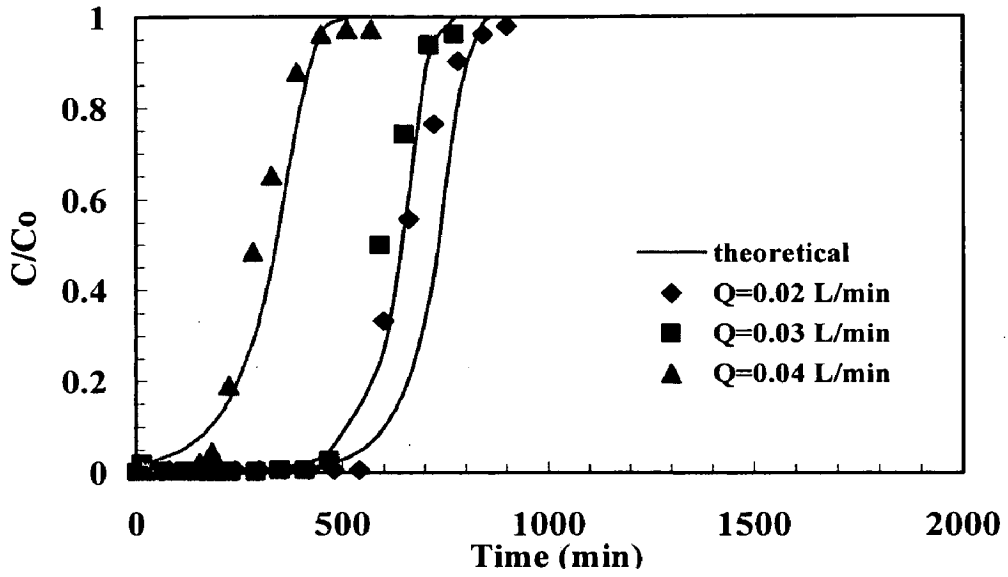

Fig. 5.34: Comparison of experimental and theoretical breakthrough curves for furfural sorption on BFA packed column using the Clark model at varied flow rates.

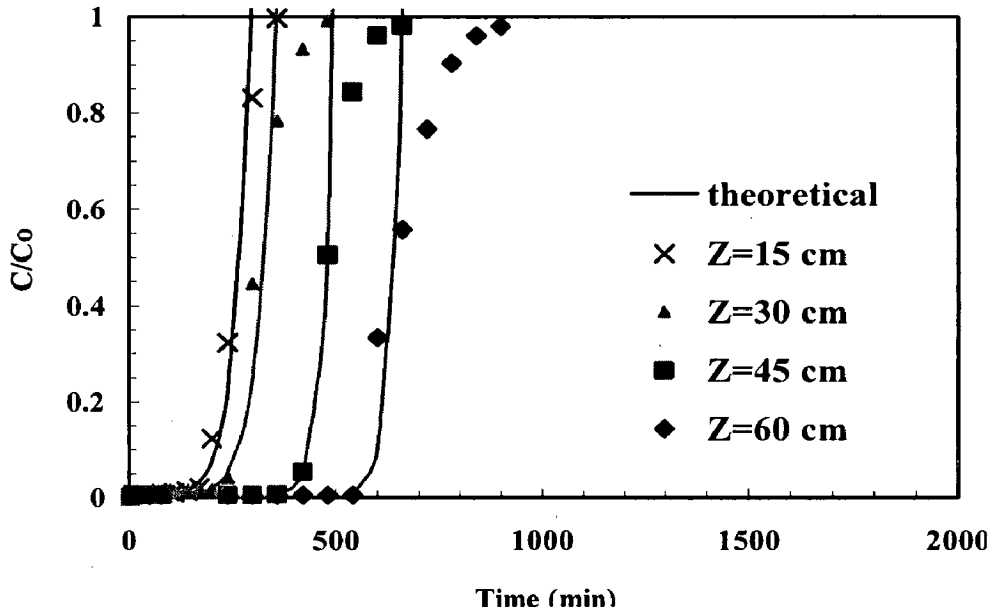

Fig. 5.35: Comparison of experimental and theoretical breakthrough curves for furfural sorption on BFA packed column using the Bohart-adams & Wolborska model at varied bed lengths.

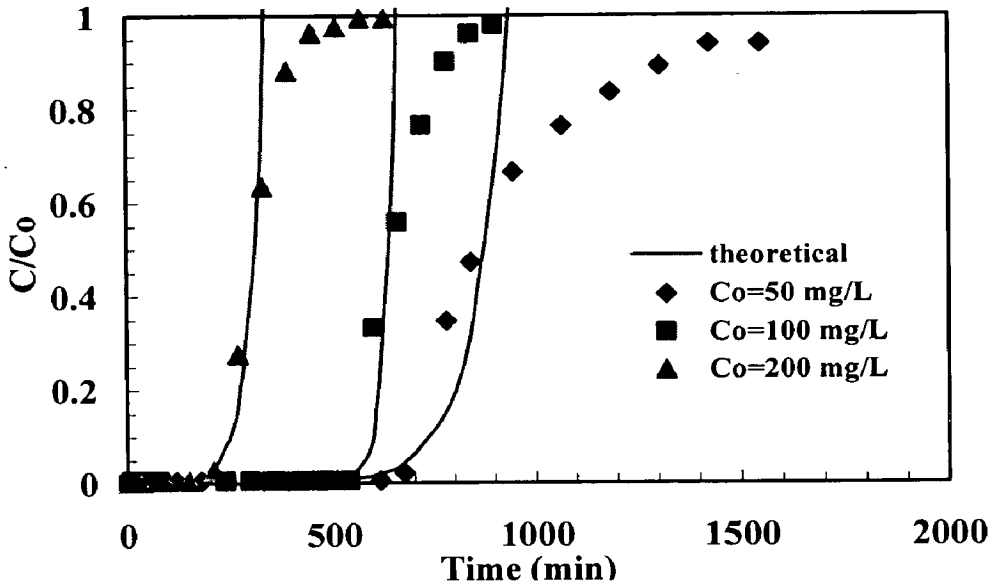

Fig. 5.36: Comparison of experimental and theoretical breakthrough curves for furfural sorption on BFA packed column using the Bohart-adams & Wolborska model at varied initial concentrations.

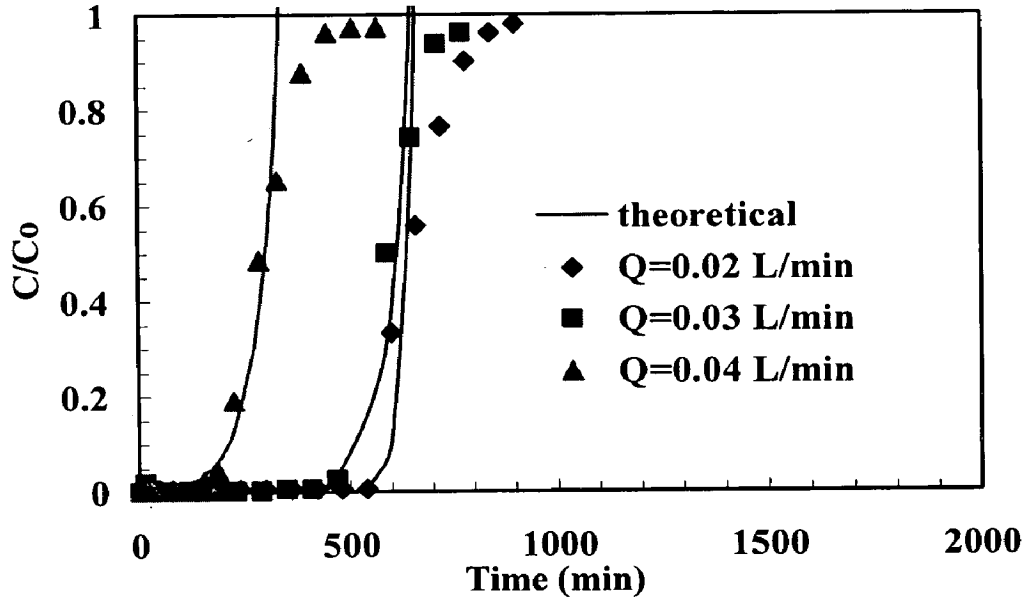

Fig. 5.37: Comparison of experimental and theoretical breakthrough curves for furfural sorption on BFA packed column using the Bohart-adams & Wolborska model at varied flow rates.

Chapter – VI

CONCLUSIONS AND RECOMMENDATIONS

7.1 CONCLUSIONS

In the present study, ACC and BFA packed bed have been used to analyze the column dynamics in the adsorption process.

For ACC packed column, the influence of the bed height (Z), inlet furfural concentration (C_o), flow rate (Q) and column diameter (D) on breakthrough curves have been investigated. Higher uptake of furfural was observed at highest Z. It was found that the value of time to breakthrough (t_b) decreased with an increase in C_o. The larger the C_o, the steeper was the slope of the breakthrough curve and smaller was the t_b. The amount of furfural adsorbed onto the unit bed height increased with an increase in Q leading to faster saturation at a higher value of Q. It was found that the adsorbent usage rate (U_r) decreased with an increase in EBCT. A 50% breakthrough curve between t and Z must result in a straight line passing through the origin, however, the straight line does not pass through the origin. The plot of 50% breakthrough ($t_{0.5}$) versus Z curve did not pass through the origin indicating the adsorption of furfural onto ACC occurs to be through complex mechanism. Adsorption capacity (N_0) as calculated from the slope of 50% plot was 7657 mg/l. Adams–Bohart, Thomas, Yoon–Nelson, Clark and Wolborska models were applied to the experimental data for the prediction of the breakthrough point. Error analysis showed that Yoon–Nelson model was most suitable for the tracing of breakthrough curve at the experimental condition.

For BFA packed column, column performance got improved with increasing Z and decreasing Q. For initial breakthrough (50%) Adam-Bohart model well predicted the breakthrough curve up to 50% breakthrough at all Z and Q. Yoon-Nelson model gave comparable values of time for 50% breakthrough point when compared with the experimental breakthrough time.

Adsorptive capacity of BFA as calculated from BDST model for 50% breakthrough plot was 3473.54 mg/l. Yoon–Nelson, Thomas, and Clark models were also applied at C/C_0 higher than 0.08 and lower than 0.99 with respect to Z and flow rate for the prediction of breakthrough curves. Model constants were determined by linear regression technique for use in the column design.

For ACC packed column, Yoon–Nelson model best described the experimental breakthrough curve, while Wolborska model showed good prediction of breakthrough curve for the relative concentration region up to 0.5. For BFA packed column, Thomas model well represented the experimental data points under all experimental conditions. Overall, more than 99.5% of furfural was removed in the column operated at an initial concentration of 100 mg/l of furfural at pH 6.5.

Overall, BFA packed column showed higher removal efficiency as compared to ACC packed column at all Q, Z and C_o.

7.2 RECOMMENDATIONS

On the basis of the present studies, BFA is recommended for the removal of furfural over ACC because of its higher removal efficiency as well as lower cost.

Pilot-scale experiment should be carried in BFA and ACC packed column for the removal of furfural from actual wastewater.

REFERENCES

1. A. Company, Furfural, general information, applications, properties, handling, Bulletin (1980) 203-D.

2. Abdulkarim M.A., Darwish N.A., Magdy Y.M., Dwaidar A., Adsorption of phenolic compounds and methylene blue onto activated carbon prepared from date fruit pits, Engineering life sciences 6 (2002) 161-165.

3. Abo-Elela S.I., El-Dib M.A., Color removal via adsorption on wood shaving, The science of the total environment. 66 (1987) 269.

4. Agrawal M., Gupta S., Project report on Studies for development of adsorption Technology for furfural removal from Aqueous streams, Department of Chemical Engineering, Indian Institute of Technology, Roorkee, India (2005).

5. Aksu Z, Gönen F, Biosorption of phenol by immobilized activated sludge in a continuous packed bed: prediction of breakthrough curves, Process biochemistry 39 (2004) 599-613.

6. Allen S.J., Gan Q., Matthews R., Johnson P.A., Comparison of optimized isotherm models for basic dye adsorption by Kudzu, Bioresource technology 88 (2003) 143-152.

7. Bailey S.E., Olin T.J., Bricka R.M., Adrian D.D., A review of potentially low-cost sorbents for heavy metals, Water research 33 (1999) 2469.

8. Belay N., Boopathy R., Voskuilen G., Anaerobic transformation of furfural by Methanococcus deltae, Applied environmental microbiology 63 (1997) 2092–2094.

9. Benjamin M., Woods S., Ferguson J., Anaerobic toxicity and biodegradability of pulp mill waste constituents, Water research 18 (1984) 601–607.

10. Bethesda M.D., Hazardous substances data bank: Furfural, NLM: National library of medicine (1992).

11. Bohart G., Adams E.Q., Some aspects of the behavior of charcoal with respect to chlorine, Journal of american chemical society 42 (1920) 523-544.

12. Borghei S.M., Hosseini S.N., Comparison of furfural degradation by different photooxidation methods, Chemical engineering journal 139 (2008) 482-488.

13. Brune G., Schoberth S., Sahm H., Growth of a strictly anaerobic bacterium on furfural (2-furaldehyde). Applied environmental microbiology 46 (1983) 1187–1192.

14. Chern J.M., Chien Y.W., Adsorption of nitrophenol onto activated carbon: isotherms and breakthrough curves, Water research 36 (2002) 647-655.

15. Cincinnati O.H., Documentation of the threshold limit values and biological exposure indices, 6th edition, ACGIH: American conference of governmental industrial hygienists [1991b].

16. Cincinnati O.H., Registry of toxic effects of chemical substances: Furfural, U.S. Department of health and human services, Public health service centers for disease control, National Institute for Occupational Safety and Health, Division of Standards Development and Technology Transfer, Technical Information Branch. (1991a).

17. Cincinnati O.H., Threshold limit values for chemical substances and physical agents and biological exposure indices, American conference of governmental industrial hygienists (1994).

18. Clark R.M., Evaluating the cost and performance of field-scale granular activated carbon systems, Environmental science & technology 21 (1987) 573.

19. Coca J., Diaz R., Extraction of Furfural from Aqueous Solutions with Chlorinated Hydrocarbons, Journal of chemical engineering data. 25 (1980) 80-83.

20. Concise International Chemical Assessment Document, 21 (2000). http://www.inchem.org/documents/cicads/cicads/cicad_21.htm

21. Cooney D.O., Adsorption Design for wastewater Treatment, Lewis Publishers, Boca Raton (1999).

22. Faust S.D., Aly O.M., Adsorption process for water treatment, Boston: Butterworths (1987).

23. Garg V.K., Gupta R., Bala A., Kumar R., Dye removal from aqueous solution by adsorption on treated sawdust, Bioresource technology 89 (2003) 121-124.

24. Goel J., Kadirvelu K., Rajagopal C., Garg V.K., Removal of lead(II) by adsorption using treated granular activated carbon: batch and column studies, Journal of hazardous material 125 (2005) 211-220.

25. Gupta M.P., Bhattacharya P.K., Studies on color removal from bleach plant effluent of a kraft pulp mill, Journal of chemical technology and biotechnology 35 (1985) 23.

26. Gupta P., Nanoti A., Garg M.O., Goswami A.N., The removal of furfural from water by adsorption with polymeric resins, Separation science and technology 36 (2001) 2835-2844.

27. Han R., Ding D., Xu Y., Zou W., Wang Y., Li Y., Zou L., Use of rice husk for the adsorption of congo red from aqueous solution in column mode, Bioresource technology, 99 (2002) 2938-2946.

28. Hathaway G.J., Proctor N.H., Hughes J.P., and Fischman M.L., Chemical hazards of the workplace, 3rd edition, New York, NY: Van nostrand reinhold. (1991).

29. Health Council of the Netherlands: Dutch Expert Committee on Occupational Standards (DECOS), Health-based recommended occupational exposure limit for furfural, The Hague Health Council of the Netherlands, draft report. (1996).

30. Ho Y.S., McKay G., Pseudo-second order model for sorption processes, Process biochemistry 34 (1999) 451-65.

31. http://dsir.nic.in/reports/techreps/tsr048.pdf

32. http://dsir.nic.in/reports/techreps/tsr048.pdf

33. http://nj.gov/health/eoh/rtkweb/0953.pdf

34. http://www.cag.gov.in/reports/commercial/2002_book3/chapter16.htm#16.2.1

35. http://www.cpcb.nic.in/standard_welcome.htm

36. http://www.inchem.org/documents/cicads/cicads/cicad_21.htm

37. http://www.jtbaker.com/msds/englishhtml/f8040.htm

38. http://www.osha.gov/SLTC/healthguidelines/furfural/recognition.html

39. Hutchins R.A., New method simplifies design of activated-carbon system Chemical Engineering 80 (1973) 133-138.

40. Kawasaki M., Experiences with the test scheme under the Chemical Control Law of Japan: An approach to structure–activity correlations, Ecotoxicology and environmental safety 4 (1980) 444–454.

41. Keith L., Chemical characterization of industrial wastewaters by gas chromatography–mass spectrometry, Science of the total environment 3 (1974) 87–102.

42. Kim T., Hah Y., Hong S., Toxic effects of furfural on Pseudomonas fluorescens, Korean journal of microbiology 21 (1983) 149–155.

43. Kumar V., Sharma S., Maheshwari R.C., Removal of COD from paper mill effluent using low cost adsorbents, Indian journal of environment protection 20 (2000) 91.

44. Lataye D.H., Mishra I.M., Mall I.D., Removal of furfural from aqueous solution by adsorption on bagasse fly ash, Industrial engineering chemical research 45 (2006) 3934-3943.

45. Lodeiro P., Cordero B., Grille Z., Herrero R., Sastre de Vicente, Physico chemical studies of cadmium (II) biosorption by the invasive alga in Europe, Sargassum muticum, Biotechnology and bioengineering 88 (2004) 237-247.

46. Lucas S., Cocero M.J., Zetzl C., Brunner G., Adsorption isotherms for ethylacetate and furfural on activated carbon from supercritical carbon dioxide, Fluid phase equilibria 219 (2004) 171–179.

47. Maarsse H., Visscher C.A., Volatile compounds in food, Sixth edition, Tno-civo Food analysis institute, Zeist, The Netherlands (1989).

48. Maga J., Furans in foods, critical review, Food science and nutrition 4 (1979) 355–399.

49. Malik P.K., Use of activated carbons prepared from sawdust and rice-husk for adsorption of acid dyes: a case study of acid yellow 36, Dyes and pigments 56 (2003) 239–249.

50. Mall I.D., Mishra N., Mishra I.M., Removal of organic matter from sugar mill effluent using bagasse fly ash activated carbon, Research and industry 39 (6) (1994) 115-119.

51. Mall I.D., Srivastava V.C., Agarwal N.K., Mishra I.M., Removal of congo red from aqueous solution by bagasse fly ash and activated carbon: kinetic study and equilibrium isotherm analyses, Chemosphere 61 (2005) 492-501.

52. Mall I.D., Srivastava V.C., Agarwal N.K., Removal of orange-G and methyl violet dyes by adsorption onto bagasse fly ash- kinetic study and equilibrium isotherm analyses, Dyes pigments 69 (2006) 210-23.

53. Mall I.D., Srivastava V.C.,. Agarwal N.K, Mishra I.M., Adsorptive removal of malachite green dye from aqueous solution by bagasse fly ash and activated carbon- kinetic study and equilibrium isotherm analyses, Colloid surface a: physicochemical engineering aspects 264 (2005) 17-28.

54. Mall I.D., Tewari S., Singh N., Mishra I.M., Utilisation of bagasse fly ash and carbon waste from fertiliser plant for treatment of furfural and 3-picoline bearing wastewater, Proceeding of The Eighteenth International Conference On "Solid waste technology and management", held at Philadelphia, PA, USA, March 23-26, 2003.

55. Mall I.D., Upadhaya S.N., Sharma Y.C., A review on economical treatment of wastewaters and effluents by adsorption, International journal of environmental studies 51 (1996) 77.

56. Namasivayam C., Radhika R., Suba S., Uptake of dyes by a promising locally available agricultural solid waste: coir pith, Waste management 21 (2001) 381.

57. Netpradit S., Thiravetyan P., Towprayoon S., Evaluation of metal hydroxide sludge for reactive dye adsorption in a fixed bed column system, Water research 38 (2004) 71-78.

58. Othmer K., Kirk-Othmer encyclopedia of chemical technology, third edition, John wiley & sons, Inc., New York (1984) 501-510.

59. Parmeggiani L., Encyclopedia of occupational health and safety, 3rd revised edition, Geneva, Switzerland: International labour organization (1983).

60. Pellizzari E., Hartwell T., Harris B., Waddell R., Whitaker D., Erickson M., Purgeable organic compounds in mothers's milk, Bulletin of environmental contamination and toxicology 28 (1982) 322–328.

61. Pitter P., Determination of biological degradability of organic substances, Water research. 10 (1976) 231–235.

62. Poots V.J.P., Mckay G., Healy J.J., The removal of acid dye from effluent using natural adsorbents-II, Wood water research 10 (1976) 1067

63. Porter J.F., McKay G., Choy K.H., The prediction of sorption from a binary mixture of acidic dyes using single- and mixed-isotherm variants of the ideal adsorbed solute theory, Chemical engineering science 54 (1999) 5863.

64. Rao J.R., Viraraghavan T., Biosorption of phenol from a aqueous solution by aspergillus niger biomass, Bioresource technology 85 (2002) 165-171.

65. Risk Assessment, Furfural CAS-No.: 98-01-1 EINECS-No.: 202-627-7 Draft of October (2004).

66. Rivard C.J., Grohmann K., Degradation of furfural (2-furaldehyde) to methane and carbon dioxide by anaerobic consortium, Applied biochemistry Biotechnology 28 (1991) 285-295.

67. Rowe E., Tullos L., Lube solvents no threat to waste treatment, Hydrocarbon processing 59 (1980) 63–65.

68. Ruus L., A study of waste waters from the forest products industry, Composition of biochemical oxygen demand of condensate from spent sulfite liquor evaporation, Svensk papperstidning 67 (1964) 221–225.

69. Sahu A.K., Mall I.D., Srivastava V.C, Studies on the adsorption of furfural from aqueous solution onto low-cost bagasse fly ash, Chemical engineering communication 195 (2008) 316.

70. Sahu A.K., Srivastava V.C, Mall I.D., Latye D.H., Adsorption of furfural from aqueous solution onto activated carbon: kinetic, equilibrium and thermodynamic study, Separation science and technology 43 (2008) 1239-1259.

71. Sharma D.C., Foster C.F., Column studies into the adsorption of chromium (VI) using sphagnum moss peat, Bioresource technology 52 (1995) 261-267.

72. Sittig M., Handbook of toxic and hazardous chemicals, 3rd edition, Park Ridge, NJ: Noyes Publications (1991).

73. Srivastava V.C., Mall I.D., Mishra I.M., Treatment of pulp and paper mill wastewaters with poly aluminium chloride and bagasse fly ash, Colloid surface a: physicochemical engineering aspects 260 (2005) 17-28.

74. Srivastava V.C., Prasad B., Mall I.D., Swamy M.M., Mishra I.M., Adsorptive removal of phenol by bagasse fly ash and activated carbon: equilibrium, kinetics and thermodynamics, Colloid surface a: physicochemical engineering aspects 272 (2006) 89-104.

75. Srivastava V.C., Prasad B., Mishra I.M., Mall I.D., Swamy M.M., Prediction of breakthrough curves for sorptive removal of phenol by bagasse fly ash packed bed, Industrial engineering chemical research 47 (2008) 1603-1613.

76. Swamy M.M., Mall I.D., Prasad B., Mishra I.M., Sorption characteristics of O-cresol on bagasse fly ash and activated carbon, Indian journal of environmental health 40 (1998) 67.

77. Thomas H.C., Heterogeneous ion exchange in a flowing system, Journal of american chemical society 66 (1944) 1664-1666.

78. Tutem E., Apak R., Unal C.F., Adsorptive removal of chlorophenols from water by bituminous shale, Water research 32 (1998) 2315.

79. Wang P., Brenchley J., Humphrey A., Screening microorganisms for uti of furfural and possible intermediates in its degradation pathway, Biotechnology letters 16 (1994) 977–982.

80. Weil J.R., Dien B., Bothast R., Hendrickson R., Mosier N.S., Ladisch M.R., Removal of biomass pretreatment fermentation inhibitors (furfural) using polymeric adsorbents, laboratory of renewable resources engineering department of agricultural and biological engineering purdue university west lafayette, IN 47907 & 2 USDA NCAUR Laboratories Peoria IL 61604 (2002).

81. Wolborska A., Adsorption on activated carbon of p-nitrophenol from aqueous solution, Water research **23** (1989) 85–91.

82. Wong Y., Yu J., Laccase catalysed decolorisation of synthetic dyes, Water research 33 (1999) 3512-20.

83. Wong Y.C., Szeto Y.S., Cheung W.H., McKay G., Adsorption of acid dyes on chitosan equilibrium isotherm analyses, Process biochemistry 39 (2004) 693.

84. Yoon Y.H., Nelson J.H., Application of gas adsorption kinetics: a theoretical model for respirator cartridge service time, American industrial hygiene association journal 45 (1984) 509-516.

85. Zulfadhly Z., Mashitah M.D., Bhatia S., Heavy metals removal in fixed bed column by macro fungus Pycnoporus sanguineus, Environmental pollution 112 (2001) 463-470.